

THE PHOTOLYSIS OF BENZOIC ACID IN THE GAS PHASE

CENTRE FOR NEWFOUNDLAND STUDIES

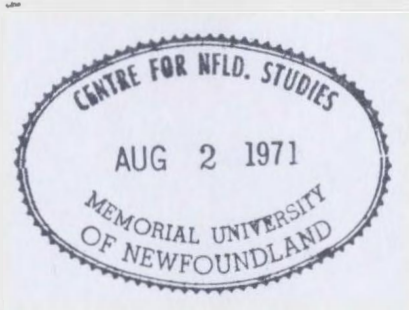
**TOTAL OF 10 PAGES ONLY
MAY BE XEROXED**

(Without Author's Permission)

FRANCIS T. C. CHAU

255656

C.1





THE PHOTOLYSIS OF BENZOIC ACID IN THE GAS PHASE

by

Francis T.C. Chau

A Thesis

Submitted to

Memorial University of Newfoundland

in partial fulfillment of the requirements

for the degree of

Master of Science

Department of Chemistry

March, 1970

ACKNOWLEDGEMENT

I would like to express my particular appreciation to Dr. D. Barton for his help and guidance in making this investigation possible. I would also like to thank deeply all those who have assisted me - Mr. C.S. Gibbons who did some preliminary experiments, Mr. D.H. Seymour for setting up part of the apparatus, Mrs. S. Banfield for drawing the diagrams and Mr. S. Chen for reading the manuscript.

I am also grateful to the National Research Council of Canada and Memorial University of Newfoundland for financial assistance.

to my mother, father
and Jean

TABLE OF CONTENTS

I.	INTRODUCTION	1
II.	EXPERIMENTAL SECTION	12
	1. General considerations	12
	2. Apparatus	17
	(i) Reactor	17
	(ii) Temperature control and thermo- couples	17
	(iii) Pressure measuring equipment	18
	(iv) Toepler pump and measured volume	20
	(v) Light source and filters	20
	(vi) Vacuum system	21
	3. Materials	21
	(i) Benzoic acid	21
	(ii) Benzene	21
	(iii) Sodium hydroxide	22
	(iv) Ethanol	22
	4. Sample introduction	22
	5. Analytical procedure	23
	6. Mass spectrometric analysis of non- condensable gases	24
	7. Gas chromatographic analysis of liquid fractions.	25
	8. Mass spectrometric analysis and titration of solid fractions	26

TABLE OF CONTENTS (Continued)

III. RESULTS	28
1. Products	28
2. Wavelength studies	29
3. Dependence of rate on light intensity	30
4. Effect of pressure	31
5. Thermal reactions	32
6. The dependence of rate upon temperature.	33
IV. DISCUSSION	38
1. Molecular structure and ultraviolet absorption spectrum of benzoic acid	38
2. Mechanisms	44
V. BIBLIOGRAPHY	59

LIST OF TABLES

1. Mass spectrometric analysis of non-condensable gases of experiment # 62	25
2. Titration of benzoic acid	27
3. Products of preliminary experiments	62
4. Effect of Corning CS 9-54 filter on the rate of CO ₂ formation	63
5. Effect of Corning CS 9-54 filter on the rate of CO formation	64
6. Effect of Corning CS 9-54 filter on the rate of H ₂ formation	65
7. Effect of intensity on rate of CO ₂ formation at 150°C	66
8. Effect of intensity on rate of CO ₂ formation at 205°C	67
9. Effect of intensity on rate of CO formation at 150°C	68
10. Effect of intensity on rate of H ₂ formation at 150°C	69
11. Effect of concentration of benzoic acid on rate of CO ₂ formation	70
12. Effect of temperature on rate of CO ₂ formation	71
13. Thermal reactions	72

LIST OF FIGURES

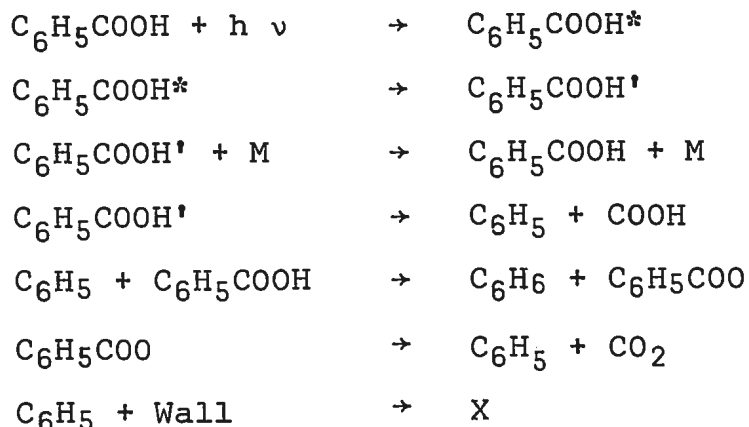
1. Diagram of apparatus	73
2. Reactor and thermocouples.	74
3. Sensing head diagram	75
4. Electronic schematic of balance unit	76
5. Optical arrangement	77
6. Percentage transmission of Corning CS 9-54 filter . .	78
7. Mass spectrum of non-condensable gases of experiment 62	79
8. Calibration chart of benzene	80
9. Plots of rates of CO ₂ and CO formation against relative light intensity at 150 and 205°C	81
10. Plots of log rate of CO ₂ formation against log relative light intensity at 150 and 205°C	82
11. Plots of log rate of CO formation against log relative light intensity at 150 and 205°C	83
12. Plots of rate of CO ₂ formation against concentration of benzoic acid at 152°C	84
13. Plots of log rate of CO ₂ formation against log concentration of benzoic acid at 152°C	85
14. Plots of log rate of CO ₂ formation against 1/T at constant light intensity and benzoic acid concentration	86
15. π -electron energy level diagram of benzoic acid . . .	87

ABSTRACT

The vapor phase photolysis of benzoic acid has been investigated in a flow system at temperatures ranging from 110° to 305°C, pressures from approximately 0.06 to 1.73 torr, and at various incident light intensities. The main identified products are carbon dioxide and benzene, and the minor identified products are carbon monoxide together with much smaller amounts of hydrogen.

At 150° and 205° the rate of formation of carbon dioxide is directly proportional to the light intensity absorbed. For a constant incident light intensity, the rate of carbon dioxide formation was found to be independent of the benzoic acid concentration at pressures from 0.29 to 1.73 torr. The rate of formation of carbon dioxide increases with temperature and the activation energy is 3.5 ± 0.4 kcal mole⁻¹.

A mechanism for carbon dioxide formation is suggested in which reaction occurs from a vibrationally excited ground state molecule, C₆H₅COOH', originating from the initially formed singlet state, C₆H₅COOH*, by internal conversion. The phenyl radical so formed initiates a free radical chain reaction.



INTRODUCTION

Although the photochemistry of aldehydes and ketones has attracted much attention, there has been comparatively little interest in the carboxylic acids. Only a few, for example formic acid, acetic acid, and butyric acid, have been investigated in the gas phase. Most aromatic acids have a low vapor pressure at room temperature. This may be the reason for the absence of any previous work on the photochemical behaviour in the gas phase of benzoic acid, or of any other aromatic acid.

A brief survey is presented of the photochemical behaviour of those acids which have been studied.

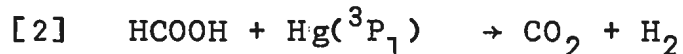
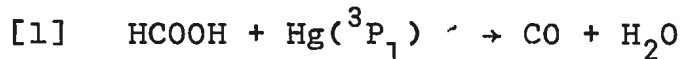
Formic Acid

Ramsperger and Porter (1), who studied the absorption spectrum of formic acid, found that monomeric and dimeric molecules existed in the vapor state and that each absorbed light below about 2600 \AA . The dimer was found to be primarily responsible for the absorption, and the monomer also had an appreciable absorption in the same wavelength range.

They exposed formic acid vapor to radiation from a quartz mercury lamp until decomposition was complete. Under these conditions the products were CO and H₂O (64%) and CO₂ and H₂ (36%). Measurements of quantum yield were not carried out.

In the Hg-photosensitized decomposition of formic

acid vapor, Bates and Taylor concluded that the reaction may occur in two ways (2)



They found that 76% of the decomposition reaction proceeded according to reaction [1'] and 24% according to reaction [2']. This is of interest since the result proves that the same quantum of energy transferred by a mercury atom can decompose a molecule in two ways. One possible explanation given by Bates and Taylor was that a steric effect may be involved in the collision of the mercury atom with the formic acid molecule; or the energy, once transferred, may be distributed in different ways among the vibrational degrees of freedom, and thus bring about two kinds of reaction.

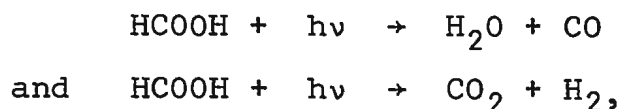
The possibility of the formation of hydrogen atoms was first pointed out by Herr and Noyes (3). They suggested that a primary decomposition into carbon dioxide and hydrogen atoms was possible



because the photon energy is of the order of 95 kcal Einstein⁻¹ and the heat of reaction is 99.9 kcal mole⁻¹. They also reported that the quantum yield for the vapor phase photolysis was slightly less than unity.

Gorin and Taylor (4), using the rate of conversion of para-hydrogen to ortho-hydrogen as an indication of the

presence of atomic hydrogen, concluded that the decomposition of formic acid was not a free radical reaction. They found that the conversion was not initiated by the decomposition of formic acid under the influence of radiation at 2000 \AA° from a zinc spark, and therefore assumed that photolysis proceeded via the reactions:

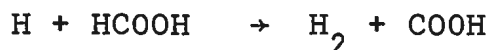


the latter becoming more important at short wavelengths. The dimeric form gave exclusively carbon dioxide and hydrogen in the wave length region from 1900 \AA° to 2540 \AA° . The total quantum yield calculated from the yield of CO plus the yield of H_2 was independent of wavelength in the range 1900 to 2540 \AA° , and was also independent of both temperature and pressure over quite considerable ranges.

On the other hand Terenin (5) later observed the spectrum of hydroxyl radical when formic acid vapor was irradiated in the far ultraviolet. This fact, of course, may have little bearing on the nature of the mechanism of photolysis at longer wave lengths.

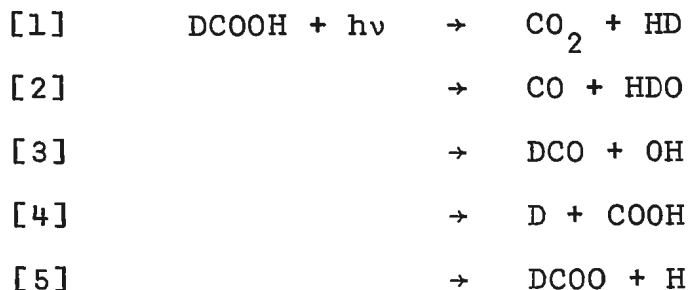
In view of the difficulty in reconciling the results of Gorin and Taylor with those of Terenin, Burton (6), using the antimony mirror method, attempted to detect hydrogen atoms in the photolysis of formic acid. He could not find any evidence for the formation of hydrogen atoms. However, in some experiments, when HCOOH was mixed with CH_3COOH in a ratio of 1 to 4, it was found that a mirror which would not last in pure acetic acid

vapor for more than about 4 minutes now took about 16 minutes to disappear. This result indicated that there could be a rapid reaction between atomic hydrogen and formic acid. Burton suggested that this reaction, for example,



was not fast enough to account for the failure to observe hydrogen atoms during the photolysis of formic acid if any were formed.

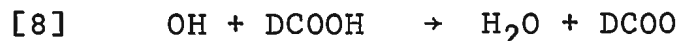
Gorden and Ausloos (8) have carried out the most detailed photochemical studies of formic acid, both HCOOH and DCOOH. They found that the yield of H₂ was, in the photolysis of DCOOH, smaller than the yield of CO₂, and that in the presence of the efficient hydrogen atom scavengers, C₂H₄ and O₂, the production of hydrogen was inhibited, whereas that of CO₂ was not affected. This clearly indicates, unlike the earlier results, that processes other than molecular reactions are involved. They considered reactions [1] to [5] as possible primary reactions in the photolysis of DCOOH.



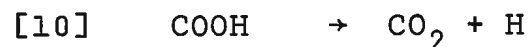
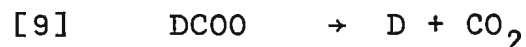
The low yields of HD relative to CO₂ indicate that process [1] cannot account for more than 5% of the overall yield.

The scavenger experiments gave evidence that only one

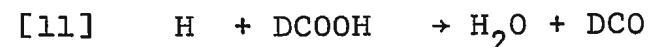
hydrogen or deuterium atom is produced for each CO₂ molecule. Therefore, the relative importance of the free radical primary processes [3], [4], and [5] can then be established on the basis of this evidence. Since processes [4] and [5] produce one hydrogen or deuterium atom for each CO₂ molecule, this is inconsistent with the results obtained. Hence, the processes [4] and [5] are believed to be unimportant at low temperatures and the results can be explained by a consideration of secondary processes involving H abstraction from DCOOH by OH,



The decomposition of DCOO and COOH may be regarded as the main source of the CO₂ at low and moderate temperature,



Furthermore, Ausloos and Gorden suggested that the hydrogen and deuterium atoms produced from the subsequent thermal decomposition of COOH and DCOO may react exclusively at low temperature by reactions [11] and [12],

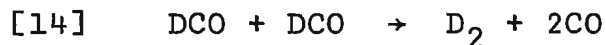


followed by



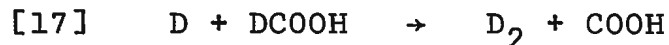
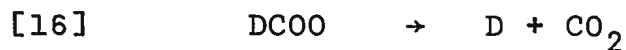
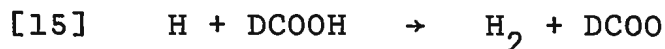
thus preventing a chain process from taking place. However,

reactions [3], [7], [8], [9], [10], [11], [12], and [13] in their proposed mechanism, clearly form a chain mechanism. If that is so, the rate of CO formation should be a function of temperature even at low temperature, which is inconsistent with the results observed. In addition, they have not mentioned any termination steps involving deuterium atoms which are produced in reaction [13]. Therefore, in order to explain the apparent absence of temperature dependence at low temperature we suggest that a possible reaction of formyl radicals is [14] instead of [13],



However, other observations suggest that the occurrence of process [2] as well as [3] is possible. For example, the yield of CO does not vary over a wide temperature range and is not affected by the presence of O_2 . Therefore, the relative importance of [2] and [3] could not be determined.

At high temperatures, they proposed that the sharp increase in the rate of formation of CO indicates that a chain reaction is taking place. The rate of CO formation in the photolysis of DCOOH is explained by reactions [11], [12] and [13]. The sharp rise in rate of production of H_2 and CO_2 also indicates the importance of chain reactions involving hydrogen atom abstraction from formic acid instead of reactions [11] and [12].



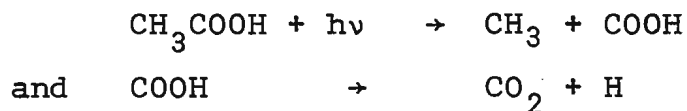
It is obvious that HD may be produced by either of the following reactions:



In the photolysis of HCOOH, the yield of H₂ was found to be smaller than the yield of CO₂. It is therefore believed that some other condensable products may have been formed besides H₂O. However, Ausloos and Gorden have not commented on this problem.

Acetic Acid

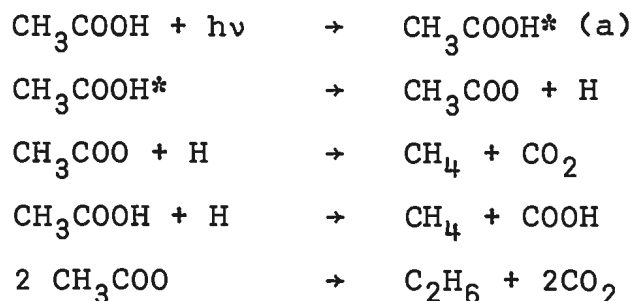
The photolysis of acetic acid vapor was studied by Burton (7,9) with the use of mirrors. He suggested that radicals were formed by the reactions



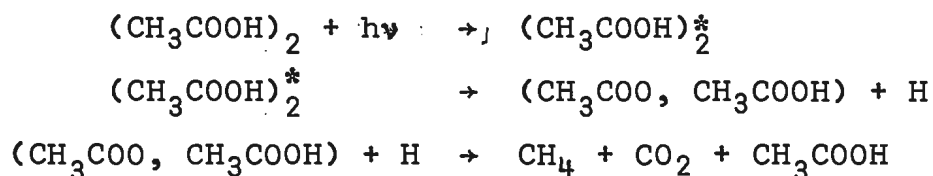
In his later work he rejected the above mechanism and suggested that hydrogen atoms were formed instead of CH₃ radicals. He, therefore, proposed the primary step to be



If the above primary process does occur, it would be necessary to postulate reactions for the CH₃COO radicals and H atoms. Burton then suggested two mechanisms to interpret his results. The one involving the monomer was



It was proposed that the dimer decomposed in a similar manner



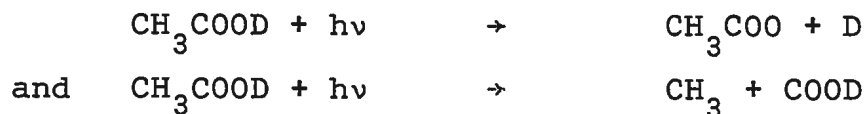
Because no information was obtained about the quantum yield as a function of the fraction of dimer present, there is no basis for choice between the two mechanisms.

Ausloos and Steacie (10) studied the photolysis of CH_3COOD . Since the rate of CH_3D formation was found to be independent of temperature, the following reaction was thought to occur

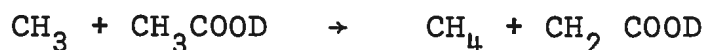


By comparing the rates of CH_3D and CO_2 formation, it was shown that this primary process accounts for only 10% of the CO_2 formed. They also reported that the rate of CO_2 formation is nearly independent of temperature over the whole range studied. This suggests the exclusion of CO_2 formation by a secondary process unless it is one with a very low activation energy. Therefore two other primary processes were proposed

(a) CH_3COOH^* represents an electronically excited molecule; and similarly elsewhere.



Since the rate of formation of CH_4 relative to the rate of formation of C_2H_6 increases rapidly with temperature they suggest that the abstraction reaction



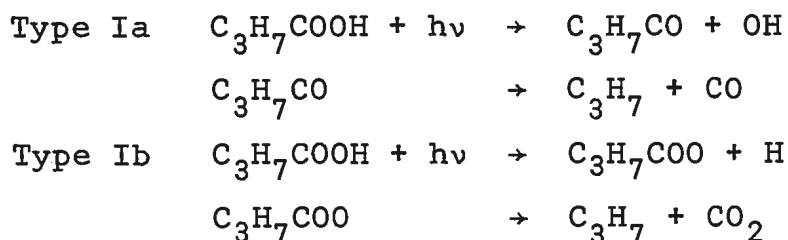
is of importance, competing with the recombination of CH_3 radicals to form ethane,



Because the rate of CO_2 formation is nearly independent of temperature, it was concluded that the primary process was the same for both dimer and monomer.

Butyric Acid

Norrish and Borrell proposed that the gaseous products of the photolysis of butyric acid (44) indicated that the primary reactions are analogous to those occurring in the aldehydes and the ketones. The Type I reactions are free radical forming, leading to carbon monoxide and carbon dioxide.



The Type II reaction is



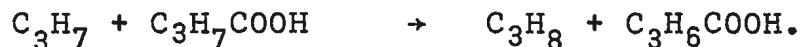
This type of reaction cannot occur unless the acid contains a γ hydrogen atom.

Because the rate of CO_2 formation is much smaller than that of methane formation in the photolysis of methyl n-butyrate in iso-octane solution, Norrish and Borrell proposed, using the assumption that acid and ester would behave similarly, that the primary reaction



does not occur, and that most of the CO_2 is formed from a type Ib reaction.

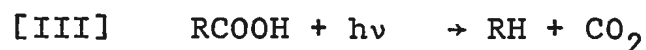
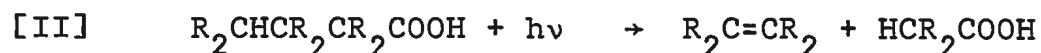
Also, the large yield of propane and the small yield of hexane indicates that hydrogen abstraction is the main reaction of the propyl radicals from the acid photolysis, i.e.



With mercury photosensitization Norrish and Wayne (45) reported that the mercury sensitized and the direct photolysis give both types of process in the same ratio. This may imply that the triplet state is the decomposing state in both types of decomposition, since the molecule is raised to a triplet state by the excited triplet state of mercury.

As Calvert and Pitts have mentioned (53), although little work has been done on the vapor phase photolysis of the acids, there is sufficient evidence to show similarity to the other carbonyls. The limited information suggests the free radical processes Ia, Ib, Ic, the Norrish type II reaction, and the intramolecular process III, for the simple acids and probably

for the more complex organic acids.



Most of the photolysis work was done at wavelengths corresponding to an excitation energy of 100 kcal mole⁻¹, considerably above that available in the thermal reactions. Hence the probability of the presence of radicals in the reaction is increased. Also benzoic acid has no hydrogen atom corresponding to the α -hydrogen required for reaction [II]. Therefore, we expect the free radical processes [Ia], [Ib], [Ic], would be of importance in our study of benzoic acid. However, the excited electronic states of formic acid and acetic acid are quite different from those of benzoic acid (this will be discussed later) possibly causing some difference in the primary processes.

In the present work an attempt is made to contribute to the understanding of the photolysis of benzoic acid in the gas phase.

EXPERIMENTAL SECTION

1. General Considerations

(1) Local and Measured Rates

As Calvert and Pitts point out (14), as long as any appreciable absorption occurs the light intensity will vary from a certain value at the front of the reaction cell to a lower value at the back of the cell. It is known that benzoic acid absorbs strongly in ethanol solution at 2280 \AA with $\epsilon_{\text{max}} = 11000 \text{ liter mole}^{-1}\text{cm}^{-1}$ (15), and radiation of this wavelength was expected to be responsible for the photochemical reaction. It is therefore clear that when a beam of light passes through benzoic acid at high pressure the absorbed light intensity will be, owing to the very large extinction coefficient, restricted to a very thin layer at the front of the reactor. Hence, the measured total or average rate of reaction cannot be treated as the local rate* in this layer at the front of the reactor. An attempt was therefore made to keep the concentration as low as possible. Calvert and Pitts have made some

* Since non-uniform light intensity is unavoidable if the reactant absorbs strongly, and if the intermediates are free radicals or atoms of short life, it may not be permissible to assume a uniform concentration. In such cases the rate equation will represent only the local reaction rate. The local rate is defined as the rate expression in an increment of volume in which the concentration of reactant and the light intensity are uniform. The equation for the overall or observed rate in the reactor as a whole must be obtained from the local rate by integration.

estimates (14) of the discrepancy between the measured and the local rates. For example, when 5, 10, 15, 20, or 50% of the incident light is absorbed in passing through a reactor, the ratios of the measured and the local rates are 1.01, 1.05, 1.62, 2.23, or 6.90 respectively, if the reaction order with respect to the absorbed light intensity is 1/2.

However, Calvert and Pitts point out that the above ratios are overestimates since there is some diffusion of radicals or reactive species from one volume element to another. Experience in a few cases has shown that if the percentage of incident light absorbed is kept below 50%, the measured and local rates will not greatly differ. Using this upper limit the desired maximum pressure was calculated by means of the Beer-Lambert Law,

$$\log \frac{I}{I_0} = \epsilon lc$$

using the extinction coefficient $\epsilon = 11000 \text{ liter mole}^{-1} \text{ cm}^{-1}$ for the 10 cm reactor.

$$\text{Thus, } c = 2.5 \times 10^{-6} \text{ mole liter}^{-1}$$

$$\text{or } p = 0.06 \text{ mm Hg at } 150^\circ\text{C.}$$

Also, from the vapor pressure data for solid benzoic acid, the vapor pressure is about 0.06 mm Hg at 65°C .

However, in a static system the percentage of reaction would be very large when the reactant pressure is about 0.06 mm Hg and a reasonable quantity of product is to be obtained. In order to have a low percentage of reaction and also to restrict the quantitative measurements to the conditions

which would minimize the errors in the rate measurements, a flow system instead of static system is desired.

All of the light intensity dependent experiments were carried out under the conditions mentioned above, and it was found that the rate of CO₂ formation is proportional to the first power of the absorbed light intensity. The local rate and the total measured rate can be written as (38)

$$\frac{d[A]}{dt \text{ local}} = \beta I_0^n (1 - e^{-\alpha c l})^n$$

$$\frac{d[A]}{dt \text{ meas.}} = \frac{\beta I_0^n (1 - e^{-\alpha c l n})}{n l (\alpha c)^{1-n}}$$

where α ($\alpha = 2.303\epsilon$) is the extinction coefficient, c the concentration, and l the length of the reactor. β is a function which includes all reactant concentrations and temperature-dependent terms and n the order with respect to the absorbed light intensity.

It is apparent that in the case of $n = 1$ the two forms become identical, i.e., if the rate of product formation is proportional to the first power of the light intensity absorbed, the measured and the local rates are equal. Therefore, reactions can be carried out at a higher concentration or pressure.

(2) Monomeric and dimeric benzoic acid

Before proceeding to do any experiments it was necessary to consider the association of benzoic acid in the vapor phase. It has been known for more than seventy years that carboxylic acids are associated in the vapor phase. The

equilibrium between monomer and dimer has been studied, and considerable quantitative data have been accumulated. Most work, however, is concerned with the aliphatic acids and the available data for aromatic acids are very scarce.

In the photolysis of formic acid, Ramsperger and Porter (1) pointed out that the monomer and dimer behave differently in the primary processes. On the other hand, Ausloos and Steacie (10) proposed that for acetic acid, dimer and monomer reacted similarly over a wide temperature range. Since it is not known how the behaviour of dimeric and monomeric benzoic acid might differ, this work was carried out at a temperature and pressure at which most of the benzoic acid was present as monomer. Allen, Watkinson, and Webb (11) have investigated the association of benzoic acid in the vapor phase by means of the infra-red carboxyl absorptions. They found the enthalpy of dimerization to be $-8.1 \text{ kcal mole}^{-1}$. However, no values of the equilibrium constant were obtained. Fortunately, Weber and Opel (12), by the vapor density method, measured the temperature dependence of the equilibrium constant for the reaction



and found the relationship

$$\log (K_p \times 10^2) = -(3.6072 \pm 0.0681) + (2.3524 \pm 0.0352) \times 10^3/T$$

In our experiments, the calculation of the percent of dimer or monomer at the experimental temperature and pressure depends on the above equation. The free energy of dimerization which they obtained is -9.726 ± 0.156 kcal mole⁻¹*

It can be calculated, using Weber's data, that at 150°C the amount of dimer would be small even for benzoic acid pressures as high as 10 mm Hg. For example, consider the monomer dimer reaction written as



When the partial pressure of each constituent is set equal to the product of its mole fraction and the total pressure P, the equilibrium constant for the reaction takes the form

$$K'_P = \frac{P_{mon.}^2}{P_{dim.}} = \frac{4\alpha^2 P}{(1-\alpha)^2} \quad \text{atm},$$

where α is the fraction of dimer dissociated at equilibrium.

At $T = 423.2$ °K, and $P = 10$ mm Hg (1.32×10^{-2} atm),

$$\log (K_P \times 10^2) = 1.953 \text{ and}$$

$$K_P = 0.898 \quad (\text{atm}^{-1})$$

$$\text{or } K'_P = 1.115 \quad (\text{atm}).$$

Thus,

$$\frac{4\alpha^2}{(1-\alpha)^2} (1.32 \times 10^{-2}) = 1.115$$

$$\alpha = 0.975$$

* The enthalpy of dimerization is -10.755 ± 0.161 kcal mole⁻¹, the entropy -25.6 ± 0.3 cal deg⁻¹ mole⁻¹.

It is apparent that 97.5% of the dimer will dissociate into monomer at a pressure of about 10 mm Hg and a temperature of 150°C. Therefore, the desired pressure range is below 10 mm Hg.

2. Apparatus

(1) Reactor

A transparent "Vitreosil" fused quartz cell, 5 cm in diameter and 10 cm in length, with polished flat quartz windows on either end was used as the reactor. Before experiment # 54 there were only two side arms connected to the reactor, 8 mm and 5 mm in outside diameter respectively, which led the fluid reactant through the reactor. After experiment # 55 a third side arm, 5 mm outside diameter, was connected to the reactor. See Fig. 2.

The reactor was placed in an aluminum block which was wound with Nichrome wire and insulated with asbestos. At one end of the block there was a double quartz window; the quartz window at the other end was insulated with asbestos. The reactor assembly was mounted in an air furnace which provided controlled temperatures up to 120°C.

(2) Temperature Control and Thermocouples

The reactor heaters were run from two 8 amp Variacs. One of them was regulated by means of a thermistor and relay. Three uncalibrated thermocouples of Chromel-Alumel in conjunction with a Leeds and Northrup Student Potentiometer were used to measure the temperature at various points on the

reactor. For details see Fig. 2. The temperature was kept constant to within $\pm 0.5^{\circ}\text{C}$ during a run.

The air furnace, with inside dimensions 25" x 30.5" x 16.5", was made of asbestos. It was divided by a partition into two compartments. The one that contained the greaseless Springham Stopcock (Springham & Co. Ltd.) was operated at about 65°C . (Hereafter this compartment is referred to as B.) The other one, compartment A, which contained the reactor, benzoic acid storage vessel and sensing head, was controlled at a higher temperature, ranging from 65°C to 120°C . The temperature was controlled by means of a Silver Spring metallic strip regulator and relay. Two uncalibrated thermocouples were used to measure the temperature in A. An electric fan was used to circulate the air in compartment A in an attempt to provide a uniform temperature.

(3) Pressure Measuring Equipment

For measuring pressure a capacitance manometer, which consists of a bakable sensing head, a balance unit and an indicator, was used. It was manufactured by the Granville-Phillips Company.

The sensing head consisted of two chambers separated by a thin metal diaphragm which was made of type 304 stainless steel. Port A (see Fig. 3) was connected directly to the middle of the reactor (see Fig. 2). Port B was connected to an auxiliary pressure measuring system. (See Figs. 1 and 3.)

The diaphragm remains in its equilibrium position as long as the pressures in both ports are equal. If the pressure in one port exceeds that in the other, the diaphragm is displaced. As the diaphragm moves relative to a fixed probe, the capacitance of the probe and the diaphragm is changed. This change in capacitance unbalances a capacitance bridge in the balance unit resulting in an AC electrical signal which is amplified, phase detected, and displayed on the indicator meter.

A schematic diagram of the sensing head and the circuit of the balance unit are shown in Figs. 3 and 4.

At the beginning of an experiment the reactor and the capacitance manometer were evacuated to a pressure below 1×10^{-4} mm Hg. When the flow of benzoic acid had begun (as described in the Sample Introduction section) the pressure was measured by leaking air into the envelope side of the sensing head until the needle on the indicator meter returned to the null position. The air pressure required to balance the capacitance manometer was measured by means of the McLeod gauge if the pressure was less than 1 mm Hg. A silicone oil manometer was used if the air pressure was between 1 and 5 mm Hg.

The pressure was measured a number of times during an experiment. For example, in # 63 a series of 7 pressure readings of benzoic acid passing through the reactor, taken successively over a period of about 40 minutes, gave the result, with average deviation, 0.216 ± 0.002 mm Hg on the most sensitive setting.

(4) Toepler Pump and Measured Volume

The toepler pump and measured volume are shown in Fig. 1.

The toepler pump was constructed by C.S. Gibbons for automatic operation. The pump was equipped with a float valve, which was surrounded by an induction coil wound on pyrex tubing. When the mercury in the pump activated the automatic relay, it also activated the induction coil which then forced the float valve down making a gas tight seal trapping some mercury above it.

The calibration of the measured volume was achieved by using a bulb of known volume. A graph of volume versus position of the mercury meniscus was prepared.

(5) Light Source and Filters

The light source was a medium pressure quartz mercury arc of Hanovia Type A (46, 47), number 637A-36. An approximately collimated beam was produced by means of two aluminum stops with 2.5 and 4 cm apertures and a quartz plano-convex lens of Spectrosil "B" glass with a focal length 200 mm. See Fig. 5 for the optical arrangement.

Power was supplied to the mercury arc by means of a Hanovia transformer, number WO 20651, with an output voltage of 280 volts.

For the light intensity dependence experiments, the beam was attenuated by means of one or two neutral density filters. The filters, which were 2" x 2" square and 1/16" thick, were obtained from the Oriel Optics Corporation as model number

G-56-72 (50% transmission) and model number G-56-74 (31.6% transmission). For two experiments, the Vitreosil window on the air furnace was replaced by a Corning glass filter CS 9-54 (# 7910) with a cutoff below 2100 \AA (Fig. 6).

(6) Vacuum System

The vacuum system was first constructed by C.S. Gibbons but most of it was modified. For details see Fig. 1.

The following accessories were used:

- (a) Fore pump -
Welch Duo-Seal, serial no. 8693-3
- (b) Diffusion pump -
Veeco, model number EP 25W
- (c) Thermocouple pressure gauge -
C.V.C., GTC-100

3. Materials

(1) Benzoic acid

Benzoic acid (The McArthur Chemical Co., number 10589811) was used with further purification. The acid was first melted and poured into a petrie dish (13). After cooling the acid was ground up in an agate mortar, placed on the vacuum line and evacuated at 0°C to remove water.

(2) Benzene

"Fisher Spectro Grade" benzene was used without any further purification.

(3) Sodium Hydroxide

This solution was made up of a "accurute" solution diluted with boiled, deionized water. The solution was usually standardized with potassium hydrogen phthalate and was stored in a polyethylene container from which carbon dioxide was excluded (48).

(4) Ethanol

95% ethanol was used without further purification.

4. Sample Introduction

Solid benzoic acid was kept in a 50 cm³ storage bulb within the air furnace. The storage bulb, kept at 0°C by a dewar which could be moved vertically by remote control, was connected directly to the reactor as shown in Fig. 1. The air furnace temperature could be adjusted to provide benzoic acid vapor at any desired pressure up to about 5 Torr. An electric fan was used to circulate the air inside the air furnace in an attempt to keep a uniform temperature throughout the box in order to prevent the condensation of benzoic acid. The temperature, measured by thermocouple, near the sensing head of the capacitance manometer was found to be around 1°C lower than that at the storage bulb.

Before an experiment was started, the bulb was held at 0°C and the bulb, the reactor, the -196°C trap, mercury diffusion pump, Toepler pump, and the gas burette were evacuated to a pressure of approximately 5×10^{-6} mm Hg. When the reactor heaters, the air furnace heaters, and the capacitance manometer

were stabilized, the ice bath was removed from the storage bulb allowing the benzoic acid to evaporate and flow from the bulb through the reactor to the trap at -196°C . The lamp was then turned on and photolysis started after allowing for a short preheating period of about 4 minutes. The pressure measurements were then carried out as described in the "Pressure Measuring Equipment" section. The photolysis time was normally about two hours.

5. Analytical Procedure

The photolysis products were separated by means of suitable cold traps into four fractions:

- (1) non-condensable gases, volatile at -196°C
- (2) CO_2 fraction, volatile at -120°C
- (3) liquid fraction, volatile at -5°C
- (4) solid fraction, volatile at 120°C .

The gases, H_2 and CO , which did not condense at -196°C , were transferred continuously during photolysis by means of the mercury diffusion pump and the automatic toepler pump into the calibrated section of the manometer. On completion of the experiment these gases were removed from the vacuum line and in most experiments were analysed by mass spectrometry.

The second fraction was Toepler pumped from the trap at -120°C into the calibrated volume, and was usually removed and scanned by mass spectrometer.

The third fraction was distilled into a sample tube for chromatographic analysis. Qualitative analysis of this

fraction was once carried out by means of mass spectrometry*, the $m/e=78$ peak in the spectrum obtained indicated the presence of benzene*. Phenol, one of the possible products, was expected to be present in the liquid fraction. However, phenol was not definitely detected. In the spectrum the ratio of the $m/e=94$ peak to the $m/e=78$ peak was about 1/150, which gives an upper limit of the rate of phenol formation of about 1×10^{-8} mole hr^{-1} .

The fourth fraction was removed by heating the trap to 120°C and distilling the contents of the removable trap. Qualitative and quantitative analysis were then carried out by means of mass spectrometry and titration.

6. Mass Spectrometric Analysis of Non-Condensable Gases

The apparatus used had been modified from a type 21-614 Residual Gas Analyser (Consolidated Electrodynamics Corporation). The background pressure was 5×10^{-8} to 1.2×10^{-7} Torr. The ionizing current was fixed at 20 micro-amperes. The input sensitivity was fixed at high and scan rate at 5.

The non-condensable gases were run through two mass ranges, the low mass range ($m/e: 2-10$) and the high mass range ($m/e: 10-150$). There was a seeming inevitable leak of air

* The contents of the trap were dissolved in 2 c.c. carbon tetrachloride and then were analysed by means of a Hitachi Perkin-Elmer RMU-6E mass spectrometer.

during photolysis from the Springham stopcocks in compartment B of the air furnace giving a mixture of CO, H₂ and air in the non-condensable gases. The compositions of the mixtures were computed. A typical instance from experiment # 62 (See Figure 7) is given below.

TABLE I
MASS SPECTROMETRIC ANALYSIS OF NON-CONDENSABLE GASES OF
EXPERIMENT # 62

	<u>H₂</u>	<u>CO*</u>	<u>N₂</u>
Basic peak	99	7105	2245
Relative sensitivity	6.5	0.99	1
Partial pressure	99 x 6.5	7105 x 0.99	2245 x 1

$$\begin{aligned} \text{Thus H}_2 : \text{CO} : \text{air} &= 99 \times 6.5 : 7105 \times 0.99 : 2245 \times 1 \\ &= 0.053 : 0.654 : 0.293 \end{aligned}$$

From these ratios the quantities of H₂ and CO could then be calculated.

7. Gas Chromatographic Analysis of Liquid Fraction

The apparatus used was a Dynatronic Instruments Chromalyzer-100 Gas Chromatograph with a thermal conductivity cell detector.

The column used was made of 3/10" O.D. copper tubing, 8" in length, and was packed with 8256-1 UCON (Dynatronic Instrument

* The calculation of the peak height of CO was based on the peak m/e = 12.

Corp., number 8231-1).

Helium, under a gauge pressure of 9.5 pounds per square inch, was used as a carrier gas. The flow rate was 35 ml per minute in the sample line and 25 ml per minute in the reference line at the operating temperature. The detector filament current was kept at 200 milliamperes and the operating temperature was adjusted to around 110°C for all runs.

Calibration for benzene was carried out at the operating conditions described above. To introduce pure benzene into the chromatograph for calibration a 5 μ l syringe (The Hamilton Company, number 2933089, 75N) was used. Several calibration points were obtained with 2.25×10^{-6} to 5.63×10^{-6} moles with attenuation settings from 2 to 8. Under the above operating conditions the retention time of benzene was found to be about 2 minutes.

The plot of the number of moles of benzene against peak area is shown in Fig. 8, and percent error was found to be about 3%.

On distillation of benzene from the trap to the sample tube, it was found that the percent of recovery was about 95%.

Attempts were made to detect water by the same method but no water was detected.

8. Mass Spectrometric Analysis and Titrations of Solid Fraction

The contents of the 120°C trap were tested for the presence of biphenyl by means of mass spectrometry (Hitachi

Perkin-Elmer RMU-6E mass spectrometer). The mass spectra were compared with a spectrum obtained from a standard mixture containing an amount of biphenyl corresponding to about 0.1% of the initial concentration of benzoic acid used in the experiment. However, it was impossible to determine whether biphenyl was present or not. This may have been due to the fact that the analysis was attempted in the presence of a large excess of the benzoic acid. The $m/e = 154$ peak appeared in the pure benzoic acid spectrum and also it was found that the spectra were not reproducible. A careful series of mass spectroscopic analysis was carried out in an attempt to detect biphenyl but it was not observed.

The unreacted benzoic acid was analysed by titration of a neutralized ethanol solution (13) of the acid with 0.01N or 0.1N sodium hydroxide solution using a Corning Model 5 pH meter (Corning Scientific Instruments).

The results of some tests of the titration method of benzoic acid analysis are given below.

TABLE II
TITRATION OF BENZOIC ACID

<u>Moles acid weighed out</u>	<u>moles titration</u>	<u>% difference</u>
$\times 10^{-4}$	$\times 10^{-4}$	
1.246	1.229	1.37
2.481	2.485	0.20
1.000	0.990	1.05
2.050	2.047	0.15

RESULTS

1. Products

The products of preliminary experiments at 150° are shown in Table III. The only identified products are carbon dioxide, benzene, carbon monoxide and much smaller amounts of hydrogen.

It can be seen in Table III that the quantity of benzene produced is always less than the quantity of carbon dioxide, but the difference is within the experimental error. The results in Table III also indicate that carbon monoxide accounts for about 10% of the total carbon dioxide plus carbon monoxide. This suggested that there must be some ring compounds other than benzene formed in the photolysis reaction. These ring compounds were expected to be phenol and biphenyl, but they were unobserved.

The percent of reaction was calculated from the quantities of carbon dioxide and carbon monoxide produced relative to the quantity of the unreacted acid, i.e.

$$\frac{\text{CO} + \text{CO}_2}{(\text{C}_6\text{H}_5\text{COOH})_{\text{unreacted}}} \times 100.$$
 This calculation is based on the assumption

that no other products are formed from -COOH except carbon dioxide and carbon monoxide. As Table III illustrates, the percent of reaction was found to be about 2% in all the experiments.

2. Wave Length Studies

Benzoic acid absorbs strongly at 2020, 2280, and 2790 A° in ethanol solution with extinction coefficients of about 8000, 11000, and 550 liter mole⁻¹ cm⁻¹ respectively (15, 19). For a particular absorption the magnitude of the molar extinction coefficient is directly proportional to the probability of the particular electronic transition. The reaction was therefore expected to be caused by the electronic excitation at wavelengths around 2280 A° . This has been confirmed by the present work.

Two experiments were made with a Corning CS 7-54 (# 7910) filter, with a cutoff below 2100 A° (See Fig. 7). This gave a rate of carbon dioxide and carbon monoxide formation approximately one-fifth of the normal rate. However, it has no effect upon the rate of hydrogen formation. The filter has a transmission of about 20% at 2280 A° and 85% at 2790 A° , and no transmission below 2100 A° . It is known that the medium pressure mercury lamp emits radiation at 2240, 2320 and 2360 A° (46, 47). These experiments, therefore, clearly show that the photochemical reaction is caused by the radiation at wavelengths around 2280 A° .

At a temperature of 175 $^\circ\text{C}$ and in a different reactor, using a static system, Gibbons (16), in a study of the direct photolysis of benzoic acid vapor, found no reaction when the Corning CS 9-54 (# 9683) filter was used. This filter has a transmission of about 80% at 2790 A° and no transmission below 2300 A° .

This is consistent with the results found in the present work.

In Tables IV, V, and VI these effects are clearly shown.

3. The Dependence of Rate on Light Intensity

In two sets of experiments, at 150°C and 205°C, the dependence of rate on light intensity was studied using neutral density filters of known transmission.

These experiments were carried out before the capacitance manometer was installed. The pressure was fixed for all of these experiments by maintaining the storage bulb temperature at 65°C. The pressure may be slightly lower than 0.06 mm Hg, the vapor pressure at 65°C, due to the pressure drop in the flow system.

The results obtained for carbon dioxide formation are shown in Table VII and Table VIII, for carbon monoxide in Table IX, and for hydrogen in Table X. The data given in these tables are presented graphically in Figures 9 to 11.

The orders of the reaction were calculated, with an Olivetti Underwood Programma 101, using the least squares treatment. The results are given below.

Reaction Orders with Respect to Light Intensity

	<u>150°C</u>	<u>204.9°C</u>
Carbon dioxide	1.058 ± 0.048	0.999 ± 0.050
Carbon monoxide	0.477 ± 0.070	0.847 ± 0.108

It can be seen from Table X that the quantities of H_2 formed in the photolysis are indistinguishable from those formed in the thermal reaction (See Table XIID). The order for the formation of CO is less than one. At $150^\circ C$ it is approximately 0.5 order, and at $205^\circ C$ it appears to be closer to one. However, the order for the formation of CO_2 has been clearly shown to be one.

4. The Effect of Pressure

The results of the study of the rate formation of carbon dioxide as a function of benzoic acid concentration, at $152.5^\circ C$, are given in Table XI. No analysis was done for non-condensable gases in any of these experiments because the mass spectrometer did not work properly at that time. Figs. 12 and 13 show the rate of carbon dioxide formation plotted against concentration of benzoic acid*. The order obtained by a least squares treatment is 0.016 ± 0.048 . The reaction order seems to be zero, although the data are quite scattered.

The scatter of the data may indicate that the reaction is sensitive to the surface of the reactor. This is consistent with the results of the light intensity experiments, explained later, which point out that the termination reaction is a wall reaction. However, the light intensity experiments

* Up to experiment # 71, experiments were carried out with Springham stopcocks. After experiment # 73 experiments were carried out using greased stopcocks.

show that the results are reproducible at low pressure. An interpretation may be that at higher pressure the surface termination step may depend on the rate of diffusion of radicals to the wall.

The rate data from runs # 63 and 64 were not used in the calculation of order. Before starting run # 63 a leak was found in the Springham stopcock which was connected directly to the reactor. It was, therefore, necessary to expose the reactor to air while repairing the leak. The data obtained in run # 63 and 64 are therefore not reliable and are rejected owing to the exposure of the reactor to air. (The effect of exposure to air will be discussed later.) The result of run # 78 is also much lower than normal; since it was very difficult to find any reasonable explanation, the result is used in the calculation of the order.

5. Thermal Reactions

Some thermal tests, with the light off, were done at the desired temperatures to look for the possible thermal reaction of benzoic acid. The gaseous products were found to be carbon dioxide, carbon monoxide, with traces of hydrogen. The results are listed in Table XIII

It can be seen from Table XIII that that the quantities of carbon monoxide and hydrogen, but not carbon dioxide, contribute significantly to the photo-reactions.

Two series of experiments, 1,2,3,4, and 11,12, were carried out successively after the reactor had been exposed to air. The quantities of carbon dioxide which were formed after the exposure were exceedingly great and gradually decreased as the experiments went on. It is, therefore, possible to say that the exposure has a crucial effect on the thermal reactions.

We assumed that there is no interaction between the photo-reaction and the thermal reaction, and the thermal correction was applied to the amounts of carbon monoxide or carbon dioxide by direct subtraction. However, see reference (50).

6. The Dependence of Rate upon Temperature

The rates of carbon dioxide formation at various temperatures ranging from 109.9 to 305.3°C were studied, and the results are listed in Table XIII. It is easy to see that the concentrations of benzoic acid were not constant at different temperatures. However, the rate of CO₂ formation is, from the pressure dependent experiments, independent of the concentration of benzoic acid which also has no effect on the temperature studies.

In Fig. 14 the logarithm of the rate is plotted as a function of 1/T. The slope of this line was estimated, by the method of least squares using an Olivetti Underwood Programma

101, to be 764 ± 92 , giving

$$\begin{aligned} E_a &= 2.303 \times 1.98 \times (764 \pm 92) \\ &= 3490 \pm 420 \text{ cal mole}^{-1}. \end{aligned}$$

Unfortunately, the preexponential factor, A, could not be estimated from the Arrhenius equation because the absolute light intensity absorbed by benzoic acid had not been measured.

It may be worth noting that the two straight lines which were obtained in the study of carbon dioxide formation at two temperatures in the light intensity experiments (Fig. 10) are almost exactly parallel. These lines could be used for the calculation of activation energy using the distance between the intersection of these straight lines with the Y axis.

Assuming that the rate expression is of the form

$$\frac{d[\text{CO}_2]}{dt} = k I_a^m [\text{C}_6\text{H}_5 \text{COOH}]^n$$

then $\log d[\text{CO}_2]/dt = \log k + n \log [\text{C}_6\text{H}_5 \text{COOH}] + m \log I_a$.

The above equation has been plotted in Fig. 10 with $\log d[\text{CO}_2]/dt$ on the Y axis and $\log I_a$ on the X axis. The slope m represents the order for the formation of carbon dioxide and the intersection of the Y axis represents the logarithm of the rate constant plus $n \log [\text{C}_6\text{H}_5 \text{COOH}]$. Then $\log k_1/k_2 = \log k_1 - \log k_2$ is the distance between the two Y intercepts from data at two different temperatures. Thus, from Fig. 10 we have

$$\log k_1 - \log k_2 = 0.145 \pm .03 *$$

Substitution of this value into the following equation

$$\log k_1/k_2 = E_a/(2.30R) \times (T_1 - T_2)/(T_1T_2)$$

gives $E_a = 2700 \pm 560 \text{ cal mole}^{-1}$.

By the same argument the activation energy for carbon monoxide formation could also be evaluated. There is, however, a small divergence in slope, and hence in the order, as shown in Fig. 11 for the formation of carbon monoxide. This divergence will greatly exaggerate the difference in rate constants at the intercept and hence the calculation of activation energy, using $\Delta \log k$, would give a misleading value.

Calculating from the data obtained from the center of the $\log I_a$ axis in Fig. 11, E_a was found to have a value of $5.1 \pm 1.3 \text{ kcal mole}^{-1}$.

Similarly, calculating for the left-hand end of the $\log I_a$ axis in Fig. 11 the following value is obtained:

$$E_a = 3.1 \pm 1.3 \text{ kcal mole}^{-1}$$

and for the right-hand end the activation energy is found to be

$$8.6 \pm 1.3 \text{ kcal mole}^{-1}.$$

No attempt was made to calculate the activation energy for hydrogen formation, because the data obtained are very scattered (See Table X).

* The value given here was corrected by considering the percentage of light absorbed at different temperatures.

It should be pointed out that in obtaining the standard deviation of the activation energy, only the errors in the rate of formation of product were taken into consideration. The errors in the measurement of the reactor temperature and the errors caused by the temperature gradient in the entrance region of the reactor could also be considered. In a flow system the temperature gradient in the entrance region of the reactor can be estimated by Leveque's formula (17, 29),

$$\frac{T - T_w}{T_\infty - T_w} = \frac{1}{0.893} \int_0^X e^{-X^3} dX$$

where X is given by

$$X = y \left(\frac{c}{9 \alpha x} \right)^{1/3}$$

$$\text{and } \alpha = \frac{k}{C_p P}$$

T is the fluid temperature, T_w the wall temperature, T_∞ the inlet temperature, k the thermal conductivity, C_p the molar heat capacity at constant pressure, P the density and c the slope of the velocity profile at the surface. c is given by $c = 2\bar{u}/d$, where d is the diameter of the reactor and \bar{u} is average flow velocity. y is the length of the reactor.

Such an estimation had been considered in our work. The thermal conductivity of benzoic acid was assumed to be about $4.0 \times 10^{-4} \text{ cal sec}^{-1} \text{ cm}^{-1} \text{ deg}^{-1}$, a typical value for molecules

of this size (49). An upper limit for the heat capacity was taken as the classical equipartition value, $83.5 \text{ cal deg}^{-1} \text{ mole}^{-1}$. Suppose the reactor temperature to be 150°C , and the pressure 0.06 torr, then

$$\alpha = 2.03 \times 10^{-3} \text{ cm}^2 \text{ sec}^{-1}.$$

The velocity \bar{u} was 0.94 cm/sec, obtained from the quantity of benzoic acid transferred as analysed by titration and calculated from $\bar{u} = w/A$ where w is the flow rate in moles per second and A is the area of the reactor cross section. Then

$$c = 0.38 \text{ sec}^{-1}$$

$$\text{and } X = 2.54 \times 10^{-2} \text{ (dimensionless)}$$

$$\text{Thus, } \int e^{-X^3} dX = 0.03.$$

The values of the integral are listed by Abramowitz (18).

It was apparent that the temperature gradient was small. For example, at $T_w = 423.2^{\circ}\text{K}$ and $T_{\infty} = 338.2^{\circ}\text{K}$,

$$T - 423.2 = 0.03 (338.2 - 423.2)$$

$$\text{and } T = 421.1^{\circ}\text{K}.$$

The errors, therefore, of temperature gradient in the reactor can then be ignored.

DISCUSSION

1. Molecular Structure and Ultraviolet Absorption Spectra of Benzoic Acid

In the wave length studies, the photochemical reaction was found to be initiated by radiation at wave lengths around 2280 \AA . (For details, see "Results" section.) It is, therefore, interesting to consider the ultraviolet absorption spectra and molecular structure of benzoic acid.

It is known that in ethanol solution benzoic acid absorbs strongly at 2020 , 2280 , and 2790 \AA , with extinction coefficients of about 8000 , 11000 , and 550 (15 , 19) respectively. In the vapor phase, we assume that the spectrum would be similar but the peak would shift to shorter wave lengths. This is supported by the behaviour of the benzene spectrum (39) as discussed below.

It is important to point out that the bands at 2280 and 2790 \AA do not correspond to transitions of the non-bonding electrons in the $-\text{COOH}$ group, but to transitions of the π -electrons of the phenyl ring. To understand this behaviour, a consideration of the molecular structure of benzoic acid is necessary. Before looking into the molecular structure of benzoic acid it is better to review briefly the quantum chemistry of the benzene molecule.

In benzene, each carbon atom is jointed to two other carbon atoms and one hydrogen atom by σ bonds forming the three sp^2 hybrid orbitals, and the bond angles are 120° . Each carbon

atom has a $p\pi$ orbital available for molecular orbital formation; and since a total of six $p\pi$ orbitals are available, six molecular orbitals are possible. The six MO's which can be obtained, by the method of group theory are (20, 42):

<u>Molecular Orbital</u>	<u>Symmetry</u>
$\psi_1 = 1/\sqrt{6} (\phi_1 + \phi_2 + \phi_3 + \phi_4 + \phi_5 + \phi_6)$	a_{2u}
$\psi_2 = 1/2 (\phi_2 + \phi_3 - \phi_5 - \phi_6)$	e_{1g}
$\psi_3 = 1/\sqrt{12} (2\phi_1 + \phi_2 - \phi_3 - 2\phi_4 - \phi_5 + \phi_6)$	e_{1g}
$\psi_4 = 1/2 (\phi_2 - \phi_3 + \phi_5 - \phi_6)$	e_{2u}
$\psi_5 = 1/\sqrt{12} (2\phi_1 - \phi_2 - \phi_3 + \phi_4 - \phi_5 - \phi_6)$	e_{2u}
$\psi_6 = 1/\sqrt{6} (\phi_1 - \phi_2 + \phi_3 - \phi_4 + \phi_5 - \phi_6)$	b_{2u}

The electronic configuration of the ground state of benzene is then $\psi_1^2 \psi_2^2 \psi_3^2$ or $a_{2u}^2 e_{1g}^4$, and since all orbitals are fully occupied, the electronic state must be a singlet and belong to the totally symmetric species, ${}^1A_{1g}$.

It is clear that the highest occupied orbitals, ψ_2 and ψ_3 , and the lowest vacant orbitals, ψ_4 and ψ_5 , are both doubly degenerate. This suggests that four lowest transitions with the same energy may be possible, and each of the excited states could be either a singlet or a triplet state. Experimentally, three different singlet states are found. If configuration interaction between electrons is taken into account the energy level is then split yielding three excited levels with different energy. By group theory these excited states are known as the ${}^1B_{2u}$, ${}^1B_{1u}$,

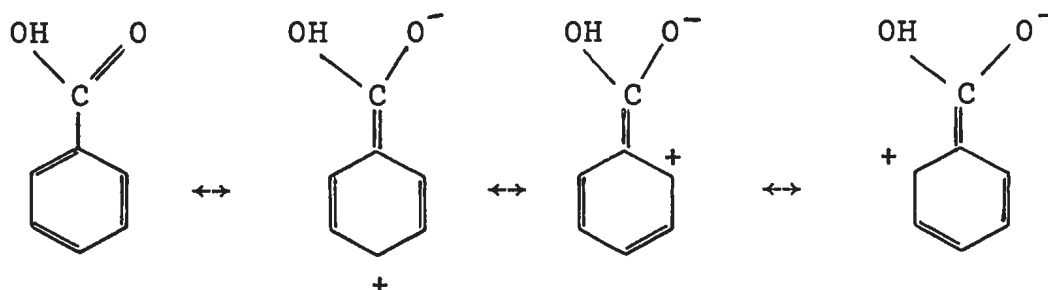
${}^1E_{1u}$. These three transitions can be assigned as the symmetry forbidden ${}^1B_{2u} \leftarrow {}^1A_{1g}$ transition at wavelength 2560 A° (39063 cm^{-1}), the forbidden ${}^1B_{1u} \leftarrow {}^1A_{1g}$ transition at 2030 A° (49261 cm^{-1}), and the allowed ${}^1E_{1u} \leftarrow {}^1A_{1g}$ transition near 1800 A° (56000 cm^{-1}).

It is known that benzene is a highly symmetrical compound, of point group D_{6h} . Most of the substituted benzenes belong to lower point groups, such as C_s and C_{2v} . However, for spectroscopic purposes, the symmetry properties of the molecule are not so important as the wave functions which are involved in the spectra. Therefore, it is convenient to describe the effect of the substituents as a perturbation. In fact, most substituent groups only slightly perturb the benzene nucleus. Substitution in benzene seldom produces great changes or new bands in the spectra, but only modifies the spectrum of the parent compound.

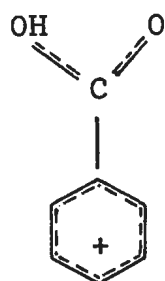
After this brief review, the discussion now centers on benzoic acid. However, the lack of understanding of this compound makes the consideration very difficult, and the following discussion is intended to be qualitative in nature.

When a carbonyl group is attached to the benzene ring the π -electron cloud of benzene is perturbed causing the spectrum to be shifted to longer wavelengths. This effect may be interpreted as a resonance interaction, which leads to a partial migration of the phenyl ring π -electrons into the substituted carbonyl group. Therefore, in terms of the resonance effect,

the substituent under consideration, $-COOH$, is regarded as an electron-withdrawing group. The π -electrons are no longer tightly held within the phenyl ring, but are more readily and extensively delocalized in the whole molecule. The resonance structures may be written as:



It is, however, possibly much better illustrated as:



The explanation of the effect of substitution may be that conjugation of the $-C = O$ with the ring causes the first bonding energy level of the π -electrons to be raised. This raising of the energy level more than compensates for the decrease of negative charge in the ring. Therefore, the benzene spectrum is shifted not to short but to long wavelength. The effect is present wherever a side chain is conjugated with the phenyl ring. Thus, phenyl cyanide, phenylethylene and benzaldehyde all show a shift to longer wavelength relative to benzene (41, 42).

On the other hand, consider Nagakura's MO approach (25). Nagakura supposes that the highest occupied orbital (H_D) of one part of the molecule (the phenyl ring) acts as electron donor in the excitation; and the lowest unoccupied orbital (V_S) of the other part (the carbonyl group) acts as the electron acceptor. He shows that H_D is higher than the highest occupied orbital of the acceptor group and that V_S is lower than the lowest unoccupied orbital of the donor group. H_D and V_S are allowed to interact with each other to form new orbitals extending over both the acceptor and donor groups, and excitation is believed to occur by promotion of an electron from the lower orbital to the higher one. On the basis of this transfer of charge, Nagakura refers to the spectra as "intramolecular charge-transfer spectra".

In order to construct a π -electron energy level diagram of benzoic acid we adapt Nagakura's approach. It is known that the $n \rightarrow \pi$ transition of acetic acid occurs at $\lambda_{\max} = 2080 \text{ \AA}$ with $\epsilon_{\max} = 32$ in ethanol solution (21), and the electron configuration of the carbonyl group in carboxylic acids has been discussed by Jaffé, Beveridge, and Orchin (22). From all the information mentioned previously a reasonable schematic π -electron energy level diagram of benzoic acid can then be constructed as shown in Fig. 15.

It seems certain that the longer wavelength band appearing at 2790 \AA is analogous to the ${}^1B_{2u} \leftarrow {}^1A_{1g}$ transition in benzene at 2560 \AA . The spectrum shows that the fine

structure vibrational bands in the parent compound are no longer present and continuous absorption bands are found instead.

The strongest absorption band, with a molecular extinction coefficient of about 11000 liter mole⁻¹ cm⁻¹, may be regarded as the intramolecular charge transfer absorption as Nagakura suggested (25). However, its origin is not yet determined conclusively; other explanations are possible. For instance, Doub and Vandenbelt (40) explained this absorption band as the shifted one of the 2030 Å⁰ band of benzene (¹B_{1u} ← ¹A_{1g}). However, the former interpretation is thought to be more reasonable (25), because the wavelength of this band is too long to be regarded as analogous to the 2030 Å⁰ band of benzene.

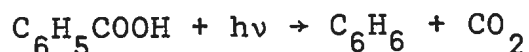
For the transition at wavelength 2020 Å⁰, the interpretation also is not clear. However, the energy level of the non-bonding electrons in the -COOH group is higher than the lowest π-electrons in benzene ring and is clearly shown in the molecular energy level diagram. This absorption band at 2020 Å⁰ may therefore be interpreted as due to the excitation of the 2p_y lone pair electrons on the oxygen atom.

Although the absorption spectrum of benzoic acid is not fully understood, it is apparent that the excited state associated with the absorption probably receives a significant contribution from a polar structure in which an electron is transferred from the aromatic ring to the conjugated substituent.

2. Mechanism for Carbon Dioxide Formation

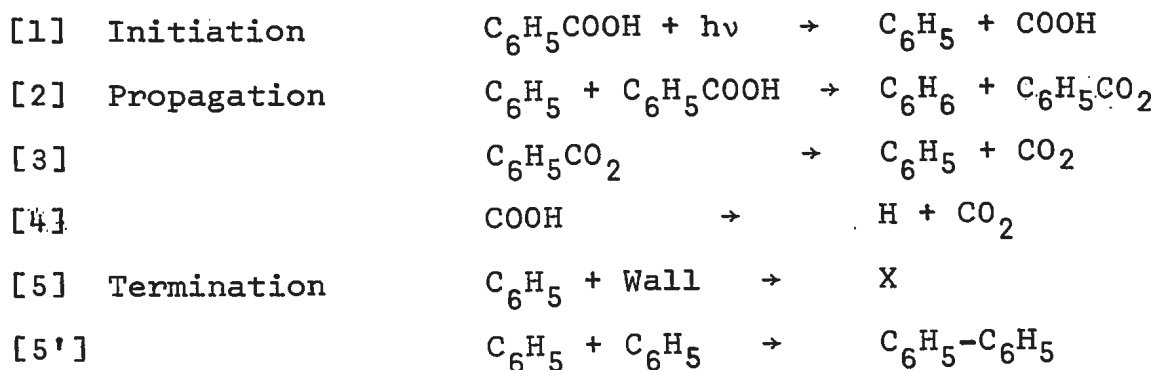
In the present study, the only identified products are carbon dioxide, benzene, carbon monoxide, and a very small amount of hydrogen. However, carbon dioxide is the only one that has been studied in detail; that is, the effects of temperature, light intensity, and pressure on the rate of carbon dioxide formation have been studied. It is, therefore, necessary to have a mechanism for carbon dioxide formation consistent with all of the observations. Before looking into the mechanism it would be better to review the steps involved in arriving at the conclusions.

Since the rate of carbon dioxide formation was found to increase slightly as the temperature was increased (the activation energy obtained in our experiments is $3.5 \text{ kcal mole}^{-1}$) the following reaction is eliminated,



because such a molecular elimination reaction would be insensitive to temperature (50).

Two chain mechanisms were therefore proposed.



Reactions [2], [3], [4], and [5'] were suggested by Winter (31) in his study of the pyrolysis of benzoic acid.

These mechanisms, with different termination steps are adapted from the mechanisms discussed by Noyes (23). He concluded that the rate of formation of products formed in the secondary reactions may display some other than first power dependence on the absorbed light intensity. In general, a recombination termination results in rate proportional to $I_a^{1/2}$, and wall termination leads to a rate which is dependent on the first power of I_a .

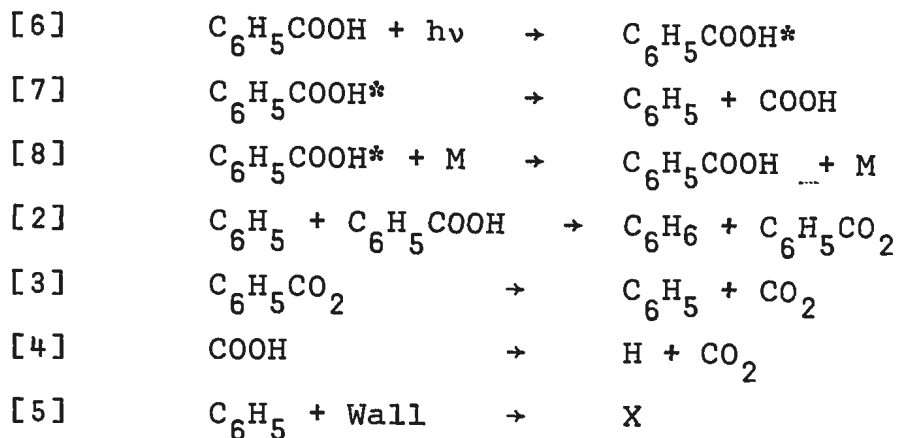
The first mechanism, with a recombination termination, leads to a rate expression for CO_2 formation which is first order with respect to the concentration of benzoic acid and one-half order with respect to the absorbed light intensity,

$$d[CO_2]/dt = (k_2/k_5') I_a^{1/2} [C_6H_5COOH].$$

The second one, with a wall termination reaction, results in the following rate expression,

$$d[CO_2]/dt = (2k_2/k_5) I_a [C_6H_5COOH].$$

The results of the light intensity experiments indicate that termination is at the wall. The first mechanism, therefore, seems to be unreasonable; however, the second mechanism is also in contradiction to the other observations found in our work. That is the rate of CO_2 formation was found to be independent of the concentration of benzoic acid. It is, therefore, suggested that deactivation of the electronically excited molecule is involved. One such mechanism is



The rate expression for CO_2 formation is then given by

$$d[\text{CO}_2]/dt = (k_7 k_2 / k_5) (I_a / k_7 + k_8 M) [\text{C}_6\text{H}_5\text{COOH}],$$

in which $M = \text{C}_6\text{H}_5\text{COOH}$. If $k_7 \ll k_8 M$,

$$d[\text{CO}_2]/dt = (k_7 k_2 / k_5 k_8) I_a [\text{C}_6\text{H}_5\text{COOH}].^{\circ}$$

This rate expression seems able to explain all of the observations, i.e. the rate of CO_2 formation is proportional to the absorbed light intensity at constant benzoic acid concentration and temperature. Also, at constant light intensity and temperature the rate of CO_2 formation is independent of the benzoic acid concentration. The temperature effect on the rate is also accounted for.

However, whether the lifetime of the electronically excited molecule, $\text{C}_6\text{H}_5\text{COOH}^*$ is long enough to undergo deactivating collisions with surrounding molecules is not known. It is, therefore, necessary to consider the lifetime of the electronically excited molecule.

An estimate of the radiative lifetime of the excited state could be obtained from the integrated area of the absorption curve using the following formula (27),

$$\tau_0 = 3.5 \times 10^8 / \nu_m^{-2} \int \epsilon dv \text{ seconds}$$

For molecules absorbing in the near ultraviolet Calvert and Pitts (28) have given the formula

$$\tau_0 = 10^{-4} / \epsilon_{\max} \text{ seconds}$$

which can be used as an approximation to estimate the radiative lifetime. As a result, the radiative lifetime of the first excited state of benzoic acid is calculated to be about 1×10^{-8} seconds with ϵ_{\max} of about 11000 liter $\text{cm}^{-1} \text{mole}^{-1}$.

Since the lifetime estimated above represents an upper limit, a comparison of the relative rates of deactivation and fluorescence can then be made, using the classical RRK theory and the kinetic theory of gases*. It was found that below a pressure of 0.1 mm Hg the rate of deactivation is much slower than the rate of fluorescence, i.e.

$$\text{Rate}_{\text{deact.}} \approx 10^{-3} \text{Rate}_{\text{fluor.}} \text{ at } 0.1 \text{ mm.}$$

Therefore the excited molecule may not last long enough to undergo deactivating collision with surrounding molecules.

However, if this mechanism is valid, the reaction rate for



* A similar calculation is given later.

must be 10^{-1} or 10^{-2} of the rate of deactivation. Therefore, the quantum yield of the reaction must be about 10^{-4} or 10^{-5} which seems to be extremely small.

Also, since the C-C bond strength in benzoic acid is 87 kcal mole⁻¹ (35, 36), and the excitation energy was 125 kcal mole⁻¹, about 40 kcal mole⁻¹ would be transferred to reaction [8] to give two ground state molecules. Whether this energy can be transferred we do not know.

Based on the considerations of lifetime, quantum yield, and energy transferred, it is more likely that the pressure effects that are observed arise from the vibrationally excited ground state molecules rather than the electronically excited molecules.

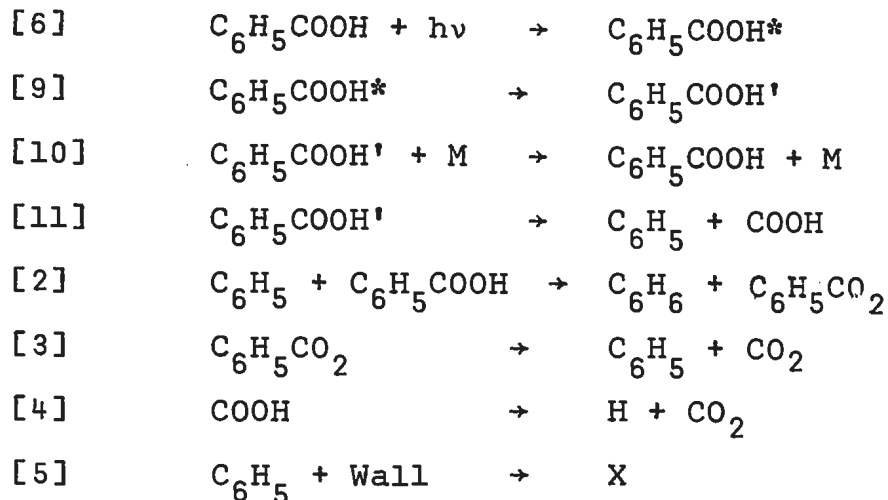
An alternate mechanism is then proposed, in which a rapid internal conversion occurs, i.e.



and reaction and deactivation take place from the vibrationally excited ground state. This type of mechanism has been proposed for other reactions, such as the photoisomerization of 1,3,5-cycloheptatriene (30, 51). In 1966 Srivivasan (43) gave a detailed discussion of the possibility of internal conversion processes. He points out that internal conversion is a common phenomenon in photochemical reactions of organic compounds. Since at total pressures of 1 to 10 mm Hg in a gaseous system, the interval between two successive collisions involving a given molecule and any other molecule is about 10^{-7} sec, it follows

that under such conditions the primary processes from the upper singlet state cannot be quenched by collisions.

Now, the proposed mechanism is written as:



In this mechanism $\text{C}_6\text{H}_5\text{COOH}^*$ represents the electronically excited molecule, $\text{C}_6\text{H}_5\text{COOH}'$ the vibrationally excited molecule in the ground electronic state, and M can be benzoic acid or any other gas.

Reactions [6], [9], and [11] are the initiation steps, and reaction [10] is the deactivation step. Reactions [2], [3], and [4] are the chain propagating steps for carbon dioxide formation, and reaction [5] is the chain termination step. By applying the steady state theory to the excited molecules and radicals, we have

$$\begin{aligned}
 I_a - k_9[\text{C}_6\text{H}_5\text{COOH}'] &= 0 \\
 k_9[\text{C}_6\text{H}_5\text{COOH}^*] - k_{10}[\text{C}_6\text{H}_5\text{COOH}'][\text{M}] - k_{11}[\text{C}_6\text{H}_5\text{COOH}'] &= 0 \\
 k_2[\text{C}_6\text{H}_5][\text{C}_6\text{H}_5\text{COOH}] - k_3[\text{C}_6\text{H}_5\text{COOH}] &= 0 \\
 k_{11}[\text{C}_6\text{H}_5\text{COOH}'] - k_2[\text{C}_6\text{H}_5][\text{C}_6\text{H}_5\text{COOH}] + k_3[\text{C}_6\text{H}_5\text{CO}_2] - k_5[\text{C}_6\text{H}_5] &= 0 \\
 \text{and } k_{11}[\text{C}_6\text{H}_5\text{COOH}'] - k_5[\text{COOH}] &= 0
 \end{aligned}$$

which can be solved to give

$$[C_6H_5CO_2] = \frac{k_{11}k_2}{k_3k_4(k_{11} + k_{10}[M])} I_a [C_6H_5COOH]$$

and $[COOH] = \frac{k_{11}}{k_4(k_{11} + k_{10}[M])} I_a$

The rate formation of carbon dioxide is

$$\frac{d[CO_2]}{dt} = k_3 [C_6H_5CO_2] + k_4 [COOH].$$

Using the expression for $[C_6H_5CO_2]$ and $[COOH]$, the following rate expression is obtained:

$$\frac{d[CO_2]}{dt} = \frac{k_{11}k_2}{k_5(k_{11} + k_{10}[M])} I_a [C_6H_5COOH] + \frac{k_{11}}{k_{11} + k_{10}[M]} I_a$$

Again, applying the long chain assumption, the second term of the above equation becomes negligible relative to the first one.

Thus,

$$\frac{d[CO_2]}{dt} = \frac{k_{11}k_2}{k_5(k_{11} + k_{10}[M])} I_a [C_6H_5COOH]$$

In order for the rate of carbon dioxide formation to be independent of benzoic acid pressure, the rate of deactivation must be much greater than the rate of reaction [11],

i.e. $k_{10}[M] \gg k_{11}$. The rate of CO_2 formation will be, if $M = \text{C}_6\text{H}_5\text{COOH}$,

$$\frac{d[\text{CO}_2]}{dt} = \frac{k_2 k_{11}}{k_{10} k_5} I_a [\text{C}_6\text{H}_5\text{COOH}]^0$$

Consequently, this equation clarifies all of the observations concerning the rate of carbon dioxide formation.

The nature of the molecule $\text{C}_6\text{H}_5\text{COOH}^*$ involved in reactions [6] and [9] must be considered. There is no evidence to suggest that the absorption of radiation by a benzoic acid molecule does not produce initially an upper electronically excited singlet state and the initially formed excited state is probably a singlet. The absorption is intense ($\log \epsilon \approx 4.0$ at 2280 \AA), and the ground state is a singlet.

The energies of the first excited singlet and triplet $\pi \rightarrow \pi^*$ electronic transitions of benzoic acid have been calculated by Fluory, Stout, and Bell (24), using the Pariser-Parr-Pople type S.C.M.O. method, to be 4.72 and 2.72 eV, respectively. The experimental value (24, 25) for the first singlet transition was found to be 4.53 eV. The experimental value for the triplet transition is still not known. There is good reason, however, to believe that a large energy difference, of the order of $46.12 \text{ kcal mole}^{-1}$, exists between the first excited singlet state and the first excited triplet state of benzoic acid. This means that intersystem crossing could be effectively eliminated. A theoretical basis for this supposition has been advanced by

Gouterman (26). It is possible that there may be a second excited triplet state between the first excited singlet state and the first excited triplet state. For purposes of discussion such a possibility has been ignored. It is assumed that only upper singlet states are involved, and also that only the first excited singlet state need be considered.

The results suggest that the deactivation reaction [10] is important, if the rate of CO₂ formation is independent of benzoic acid pressure. The relative rates of reactions [10] and [11] may be estimated by applying the classical RRK theory and the kinetic theory of gases. The rate of decomposition and the rate of deactivation of the vibrationally excited ground electronic state molecule, C₆H₅COOH', are

$$-\frac{d[\text{C}_6\text{H}_5\text{COOH}']}{dt} \text{ decomp.} = \nu \left(1 - \frac{E^*}{E}\right)^{s-1} [\text{C}_6\text{H}_5\text{COOH}']$$

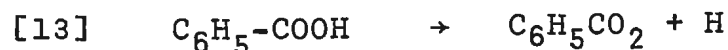
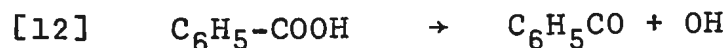
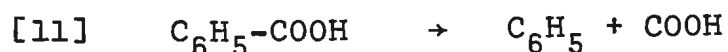
$$-\frac{d[\text{C}_6\text{H}_5\text{COOH}']}{dt} \text{ deact.} = \lambda[M] [\text{C}_6\text{H}_5\text{COOH}']^2 \sigma \left(\frac{8kT}{\mu}\right)^{1/2}$$

The frequency factor is assumed to be 10¹⁴ sec⁻¹, and the critical energy E* is approximately 86.9 kcal mole⁻¹, from the heat of reaction. The energy E is approximately 125.4 kcal mole⁻¹, calculated from the wave length 2280 Å°. The

number of oscillators, s is assumed to be 20, by taking s as equal to one half of the total number of normal modes in the molecule (33). The assumed value of the collision efficiency λ is 1* and of the collision cross section σ is 7 \AA^{**} , while the temperature is set at 150.0°C .

If the rate of deactivation and the rate of decomposition are equated, $[M]$ may be calculated to be 1×10^{-3} mm Hg. Clearly, it can be seen that the rate of deactivation will be much greater than the rate of decomposition at 0.06 or 1.73 mm Hg. This would be so even if the collision efficiency were decreased to say 1/10, i.e. if the energy is transferred by 10 or more collisions, the deactivation process [10] is still important.

The energy corresponding to 2280 \AA^0 is $125.4 \text{ kcal einstein}^{-1}$ which is more than enough to break any of the bonds $\text{C}_6\text{H}_5\text{-COOH}$, $\text{C}_6\text{H}_5\text{CO-OH}$, or $\text{C}_6\text{H}_5\text{COO-H}$. The energies of these bonds can be estimated from the tables of Benson (35) and of Cox (36) as $86.9 \text{ kcal mole}^{-1}$ for the first, and by analogy with acetic acid, 109.1 and $110.8 \text{ kcal mole}^{-1}$ for the second and third respectively. Therefore, the following reactions

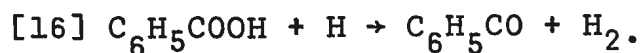
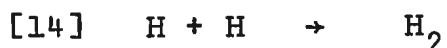


are possible.

* It is assumed that deactivation occurs at each collision.

** Mack (34) has reported a diameter of 5.7 \AA^0 for the benzene molecule. The diameter of the benzoic acid molecule cannot be much greater than this value.

It is possible to establish the relative importance of the above dissociation processes by considering the succeeding secondary processes. The yield of hydrogen is extremely small relative to that of the other products. This may indicate that reaction [13] is relatively unimportant. One may also treat as unimportant all those reactions producing H₂ or H atoms as shown below.



Reaction [12] followed by [17] (other reactions will be discussed below), may be considered for the formation of CO,



which constitutes 10% of the carbon oxides since the ratio [CO]/[CO + CO₂] is about 0.10.

However, a consideration of the energies involved shows that of the three dissociation reactions of C₆H₅COOH', reaction [11] must predominate. This may be clearly shown by estimating (52) the rate k* (E) of a unimolecular reaction (52) with an activation energy E* which is given by

$$k^* (E) = \bar{v} \left(1 - \frac{E}{E^*}\right) s^{-1}$$

If we consider the relative rates of [11], [12], and [13], at some energy, for example E*₁₁ = 87 kcal mole⁻¹, E*₁₂ = 110 kcal mole⁻¹, E = 125 kcal mole⁻¹, s₁₁ = s₁₂ = 20 (33),

* The value of E*₁₂ is the average for D(C₆H₅CO-OH) and D(C₆H₅COO-H).

and $v_{11} = v_{12}$, then

$$k_{11}/k_{12} = 10^5.$$

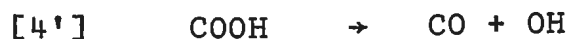
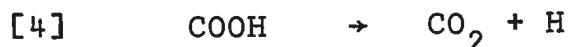
This estimate is admittedly quite approximate but it seems safe to infer that for photon energies of the magnitude used here the estimate is reasonable. Hence reaction [12] is unimportant relative to reaction [11]. Also, a negligible quantity of the carbon dioxide can be formed via reaction [13].

The large yield of benzene indicates that the hydrogen abstraction reaction [2], $C_6H_5 + C_6H_5COOH \rightarrow C_6H_6 + C_6H_5CO_2$, is the main reaction of phenyl radicals.

It is known that carboxyl radicals, $RCOO$, are very unstable toward decomposition (37); therefore reaction [3] is reasonable.

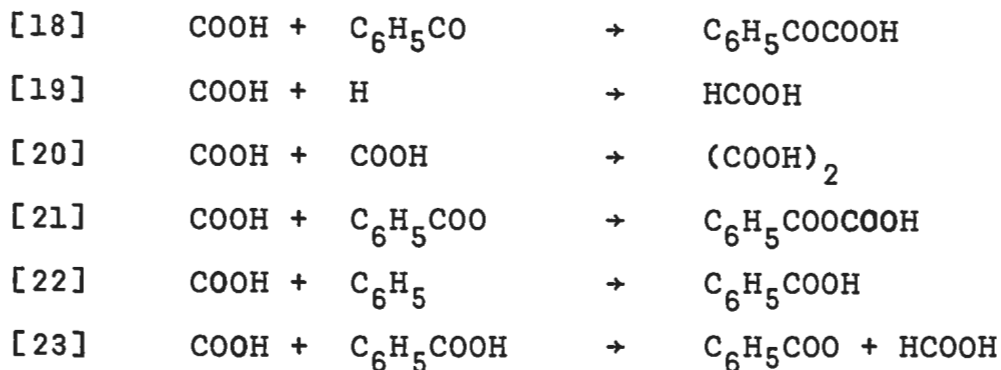


As for $COOH$, there are two possible decomposition reactions,



The heats of reaction ΔH have been estimated to be 20 kcal mole⁻¹ and 45 kcal mole⁻¹ by Back and Sehon (32) and to be 1 and 26 kcal mole⁻¹ by Gorden and Ausloos (8) respectively. No matter which values are accepted reaction [4'] will always be 25 kcal mole⁻¹ more endothermic than reaction [4]. It may be assumed, therefore, that the decomposition reaction ought to be

reaction [4] rather than [4']. Owing to the fact that COOH, as well as $C_6H_5CO_2$, are probably too unstable to take part in reactions other than decomposition, then the following reactions can also be neglected.



On the other hand, in the study of the thermal decomposition of phenylacetic acid (32), oxalic acid was suggested as one of the possible products under certain conditions. Also, Winter (31) suggested that formic acid was a product in the pyrolysis of benzoic acid in the vapor phase. Therefore, reactions [19] and [20] may occur.

During the study of the effect of pressure on rate, no analysis of carbon monoxide or hydrogen was carried out (See Experimental section). Because of this, no definite conclusions can be arrived at concerning the mechanism of carbon monoxide and hydrogen formation. However, from the intensity dependence experiments some suggestions can be made.

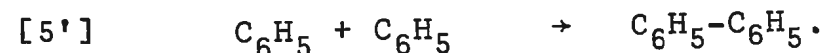
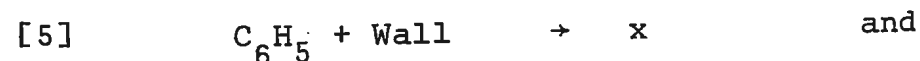
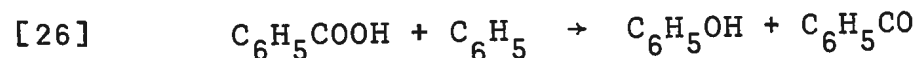
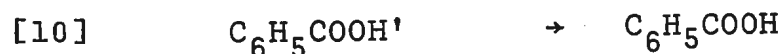
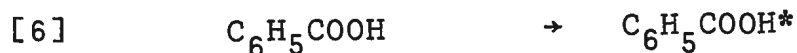
As shown in the section on results, the activation energy for CO formation is about $7.0 \text{ kcal mole}^{-1}$. It may be concluded that the following elimination reactions



do not contribute significantly to the formation of carbon monoxide. In the consideration of the relative rates of reactions [11] and [12] it was shown that reaction [12] is relatively unimportant. For this reason reaction [12], followed by [17] is not a possible source of CO.



The activation energy for CO formation, however, may be interpreted in terms of a chain mechanism. For example, consider the mechanisms given below.



The reaction orders for CO formation with respect to light intensity at 150° and 205° C are found to be 0.49 and 0.85 respectively. The order of reaction is definitely less than 1, indicating that

the recombination reaction [5'] is competing with the first order wall termination step [5] but that the homogeneous recombination reaction is predominant. The perfect order, 0.5, is seldom found in long-chain radical reactions (53) because some degree of termination usually takes place by the reaction of the chain carriers with impurities or at the wall of the reaction cell. The above mechanism is similar to that proposed for the formation of CO_2 except that in the case of CO_2 the wall termination reaction [5] is required. This is in contradiction to the results obtained for the formation of CO. It is believed therefore that some other mechanism is responsible for CO formation.

As for hydrogen, in addition to the extremely small quantity produced, the scatter of the results in the light intensity experiments, and the lack of knowledge on the pressure dependence gives us no way of determining the mechanism of its formation.

BIBLIOGRAPHY

1. H.C. Ramsperger and C.W. Porter. J. Am. Chem. Soc. 48, 1267 (1926).
2. R. Bates and H.S. Taylor. J. Am. Chem. Soc. 49, 2438 (1927).
3. W.N. Herr and W.A. Noyes Jr. J. Am. Chem. Soc. 50, 2345 (1928).
4. E. Gorin and H.S. Taylor, J. Am. Chem. Soc. 56, 2042 (1934).
5. Terenin, Acta Physicochim. U.R.S.S., 3, 181 (1935).
6. M. Burton. J. Am. Chem. Soc. 58, 1655 (1936).
7. M. Burton, J. Am. Chem. Soc., 58, 1645 (1936).
8. R. Gordien and P. Ausloos. J. Phys. Chem. 65, 1033 (1961).
9. M. Burton, J. Am. Chem. Soc. 58, 692 (1936).
10. P. Ausloos and E.W.R. Steacie, Can. J. Chem. 33, 1530 (1955).
11. G. Allen, J.G. Watkinson and K.H. Webb. Spectrochimica Acta. 22, 807 (1966).
12. G. Opel and U.V. Weber. Z. Chem. 6, 349 (1966).
13. I.M. Kolthoff and E.B. Sandell. Textbook of Quantitative Inorganic Analysis, MacMillan, N.Y., p 525, 1936.
14. J.G. Calvert and J.N. Pitts Jr. Photochemistry, John Wiley and Sons Inc. 1967, p 641.
15. A.I. Scott. Interpretation of the U.V. Spectra of Natural Products, Pergamon, Oxford., 1964, p.116.
16. C.S. Gibbons. Photochemical Studies of Benzoic Acid, Bachelor of Science Thesis, Memorial University of Newfoundland, 1966.
17. Leveque. Ann-Mines (12) 13, 201, 305, 381 (1928).
18. M. Abramowitz. J. Math. and Phys, 30, 162 (1951).
19. C.M. Moser and A.I. Kohlenberg. J. Chem. Soc. 804 (1951).
20. C. Sandorfy. Electronic Spectra and Quantum Chemistry, Prentice-Hall Inc., 1964, p 196.

21. J.G. Calvert and J.N. Pitts Jr. Photochemistry, John Wiley and Sons Inc., 1967, p 428.
22. H.H. Jaffé, D.L. Beveridge and M. Orchin. J. Chem. Ed. 44, 383 (1967).
23. W.A. Noyes, Jr. and P.A. Leighton. The Photochemistry of Gases, Dover Publications, Inc., N.Y. 1940, p 195.
24. R.L. Flurry, Jr., E.W. Stout and J.J. Bell. Theoret. Chim. Acta. 8(3), 203 (1967).
25. S. Nagakura and J. Tanaka. J. Chem. Phys. 22, 236 (1954) and S. Nagakura. J. Chem. Phys. 23, 1441 (1955).
26. M. Gouterman. J. Chem. Phys. 36, 2846 (1962).
27. N.J. Turro, Molecular Photochemistry, W.A. Benjamin Inc., 1967, p 48.
28. J.G. Calvert and J.N. Pitts, Jr. Photochemistry, John Wiley and Sons Inc., 1967, p 280.
29. H. Melville and B.G. Gowenlock. Experimental Methods in Gas Reactions, MacMillan and Co. Ltd., 1964, p 24.
30. R. Srinivasan. J. Am. Chem. Soc. 82, 3432 (1962).
31. G.K. Winter. The Gas Phase Thermal Decomposition of Benzoic Acid, Master of Science Thesis, Memorial University of Newfoundland, 1967.
32. M.H. Back and A.H. Sehon. Can. J. Chem. 38, 1261 (1960).
33. K.J. Laidler, Chemical Kinetics, 2nd ed., McGraw-Hill Book Co. Inc., N.Y., 1965, p.149.
34. E. Mack Jr. J. Am. Chem. Soc. 47, 2468 (1925).
35. S.W. Benson, J. Chem. Ed. 42, 502 (1965).
36. J.D. Cox. Tetrahedron 18, 1337 (1962).
37. J.G. Calvert and J.N. Pitts, Jr. Photochemistry, John Wiley and Sons Inc., 1967, p 430.
38. J.G. Calvert and J.N. Pitts, Jr., Photochemistry, John Wiley and Sons Inc., 1967, p 640.
39. J.R. Dyer. Applications of Absorption Spectroscopy of Organic Compounds, Prentice-Hall Inc., 1965, p 17.

40. L. Doub and J.M. Vandenbelt. J. Am. Chem. Soc. 69, 2714, (1947).
41. W.W. Robertson, J.F. Music and F.A. Matsen. J. Am. Chem. Soc. 72, 5260 (1950).
42. A.D. Baker, C.R. Brundle, and D.W. Turner. J. Mass Spectromy and Ion Phys., 1, 443 (1968).
43. R. Srinivasan. Advances in Photochemistry, ed. W.A. Noyes Jr., G.S. Hammond, and J.N. Pitts Jr., Vol. 4, New York: Interscience, 1966 p 113.
44. P. Borrell and R.G.W. Norrish. Proc. Roy. Soc. A262, 19 (1961).
45. R.G.W. Norrish and R.P. Wayne. Proc. Roy. Soc. A284, 1 (1965).
46. J.G. Calvert and J.N. Pitts Jr. Photochemistry. John Wiley and Sons, Inc., 1967 p 696.
47. Hanovia Lamp Division, Research Laboratory 5-1-59, Form EH-223.
48. I.M. Kolthoff and E.B. Sandell, Textbook of Quantitative Inorganic Analysis. Macmillan, N.Y. 1936, p 527.
49. Handbook of Chemistry and Physics, 48th Edition, The Chemical Rubber Co., 1968, E-4.
50. J.G. Calvert and J.N. Pitts Jr. Photochemistry, John Wiley and Sons, Inc., 1967, p 645.
51. N.J. Turro, Molecular Photochemistry. W.A. Benjamin Inc., 1967, p 188.
52. R. Srinivasan. J. Am. Chem. Soc. 91, 7557 (1969).
53. R.J. Field and P.I. Abell. J. Am. Chem. Soc. 91, 7226 (1969).

TABLE III

Products of preliminary experiments

Run	Temperature (°C)	Time (sec)	moles x 10 ⁶				Benzoic acid transferred	$\frac{\text{CO}}{\text{CO} + \text{CO}_2} \times 100$	% of reaction
			CO ₂	CO	H ₂	C ₆ H ₆			
32	150.8	8133	1.797	0.259	0.049	2.110	145.0	12.6	1.42
33	150.5	7511	1.777	0.254	0.046	1.996	143.0	12.5	1.42
34	150.1	7571	1.607	0.191	0.032	1.731	106.5	10.6	1.69
35	149.9	7572	1.695	0.209	0.037	1.430	110.9	11.0	1.72
36	150.5	7592	1.714	0.214	0.034	1.857	144.2	11.1	1.34
37	150.1	7571	1.588	0.161	0.029	1.526	134.5	9.0	1.37
38	150.0	7572	1.487	0.157	0.024	1.426	098.0	9.5	1.69
39	150.2	7591	1.553	0.172	0.028	1.719	149.6	10.0	1.15
Thermal Test	150.2	7571	0.080	0.020	0.017	—	118.6	20.0	0.10

— No analysis performed.

TABLE IV

Effect of Corning CS 9-54 filter on the rate of formation of CO₂ at 205°C and relative intensity = 1

<u>Run</u>	<u>Pressure (mm Hg)</u>	<u>[C₆H₅COOH]x10⁵ (moles liter⁻¹)</u>	<u>Time (sec)</u>	<u>Filter</u>	<u>R_{CO₂} x10⁶ (mole hr⁻¹)</u>
54	0.091	0.305	7487	none	1.371
55	0.095	0.319	7200	CS 9-54	0.306
56	0.093	0.312	7209	CS 9-54	0.312
57	0.107	0.359	7204	none	1.850
58	0.095	0.319	7200	none	1.490

Average rate with filter = 0.31

Average rate without filter = 1.57

TABLE V

Effect of Corning CS 9-54 filter on the rate of formation of CO at 205°C and relative intensity = 1

<u>Run</u>	<u>Pressure (mm Hg)</u>	<u>[C₆H₅COOH] x 10⁵ (mole liter⁻¹)</u>	<u>Time (sec)</u>	<u>Filter</u>	<u>R_{CO} x 10⁷ (mole hr⁻¹)</u>
54	0.091	0.305	7487	none	2.36
55	0.095	0.319	7200	CS 9-54	0.87
56	0.093	0.312	7209	CS 9-54	0.78
57	0.107	0.359	7204	none	3.05
58	0.095	0.319	7200	none	3.28

Average rate with filter = 0.83

Average rate without filter = 3.23

TABLE VI

Effect of Corning CS 9-54 filter on the rate of formation of H₂ at 205°C and relative intensity = 1

<u>Run</u>	<u>Pressure (mm Hg)</u>	<u>[C₆H₅COOH] x 10⁵ (mole liter⁻¹)</u>	<u>Time (sec)</u>	<u>Filter</u>	<u>R_{H2} x 10⁸ (mole hr⁻¹)</u>
54	0.091	0.305	7487	none	1.22
55	0.095	0.319	7200	CS 9-54	1.26
56	0.093	0.312	7209	CS 9-54	1.14
57	0.107	0.359	7204	none	1.71
58	0.095	0.319	7200	none	1.91

Average rate with filter = 1.20

Average rate without filter = 1.61

TABLE VII

Effect of intensity on rate of formation of carbon dioxide at 150°C and pressure \approx 0.065 mm Hg (A)

Run	Relative Intensity	Time (sec)	$R_{CO_2} \times 10^6$ (mole hr ⁻¹)	$\log_{10} R_{CO_2}$	\log_{10} (Relative Intensity)
41	1	7571	—	—	0
42	1	7571	1.315	-5.8811	0
43	0.316	7574	0.426	-6.3706	-0.5003
44	0.15	7571	0.179	-6.7471	-0.8239
45	0.5	7572	0.658	-6.1818	-0.3010
46	0.316	7850	0.416	-6.3809	-0.5003
47	1	7571	1.231	-5.9098	0

(A) The pressure of benzoic acid was only known approximately from the vapor pressure data.

— No analysis performed.

TABLE VIII

Effect of intensity on rate of formation of carbon dioxide

Run	Pressure (mm Hg)	[C ₆ H ₅ COOH] x 10 ⁵ (mole liter ⁻¹)	Temperature (°C)	Relative Intensity	Time (sec)	R _{CO₂} x 10 ⁶ (mole hr ⁻¹)	log ₁₀ R _{CO₂}	log ₁₀ (Relative intensity)
48			200.0	1	3600	1.824	-5.7390	0
49			200.0	1	5400	1.806	-5.7435	0
50			200.0	0.15	7200	0.231	-6.6384	-0.8239
51			200.0	0.3	5400	0.590	-6.2291	-0.5003
52			200.0	0.3	7200	0.561	-6.2510	-0.5003
53 (a)			200.0	0.3	7200	0.455	-6.3420	-0.5003
54	0.091	0.305	204.9	1	7487	1.371	-5.8630	0
57	0.107	0.359	204.9	1	7204	1.856	-5.7314	0
58	0.095	0.319	204.9	1	7200	1.490	-5.8628	0
59	0.085	0.286	204.9	0.15	7200	0.245	-6.6108	-0.8239
60	0.088	0.296	204.9	0.5	7200	0.840	-6.0757	-0.3010
61	0.085	0.286	204.9	0.3	7200	0.565	-6.2483	-0.5003

(a) From # 48 to 53 the pressure of benzoic acid was only known approximately from the vapor pressure data.

TABLE IX

Effect of intensity on rate of formation of carbon monoxide

Run	Pressure (mm Hg)	[C ₆ H ₅ COOH] x 10 ⁵ (mole liter ⁻¹)	Temperature (°C)	Relative Intensity	Time (sec)	R _{CO} x 10 ⁷ (b) (moles hr ⁻¹)	log ₁₀ R _{CO}	log ₁₀ (Relative intensity)
41			150.0	1	7571	1.370	-6.9910	0
42			150.0	1	7571	0.950	-7.0223	0
43			150.0	0.3	7475	0.525	-7.2999	-0.5003
44			150.0	0.15	7571	0.320	-7.4949	-0.8239
45			150.0	0.5	7571	0.620	-7.2076	-0.3010
46			150.0	0.3	7572	0.552	-7.2581	-0.5003
47(a)			150.0	1	7580	—	—	0
48-53(c)								
54	0.091	0.305	204.9	1	7487	1.930	-6.7144	0
57	0.107	0.359	204.9	1	7204	2.620	-6.5817	0
58	0.095	0.319	204.9	1	7200	2.850	-6.5452	0
59	0.085	0.286	204.9	0.15	7200	0.442	-7.3546	-0.8239
60	0.088	0.296	204.9	0.5	7200	1.390	-6.8570	-0.3010
61	0.085	0.286	204.9	0.3	7200	1.160	-6.9355	-0.5003

(a) The initial pressure of benzoic acid was only known approximately from the vapor pressure data.

(b) A thermal correction was applied to the amounts of carbon monoxide formed.

(c) From # 48 to # 53 no attempt was made to analyse the carbon monoxide.

— No analysis performed.

TABLE X

Effect of intensity on rate of formation of hydrogen

Run	Pressure (mm Hg)	[C ₆ H ₅ COOH] x 10 ⁵ (mole liter)	Temperature (°C)	Relative Intensity	Time (sec)	R _{H₂} x 10 ⁸ (b) (mole hr ⁻¹)
41			150.0	1	7571	1.970
42			150.0	1	7571	1.940
43			150.0	0.3	7574	1.172
44			150.0	0.15	7571	0.991
45			150.0	0.5	7571	1.703
46			150.0	0.3	7572	1.312
47 (a)			150.0	1	7580	—
48-53 (c)						
54	0.091	0.305	204.9	1	7487	1.225
57	0.107	0.359	204.9	1	7204	1.710
58	0.095	0.319	204.9	1	7200	1.913
59	0.085	0.286	204.9	0.15	7200	0.620
60	0.088	0.296	204.9	0.5	7200	1.370
61	0.085	0.286	204.9	0.3	7200	1.453

(a) The pressure of benzoic acid was only known approximately from the vapor pressure data.

(b) No thermal correction was applied to the amounts of hydrogen formed.

(c) From #48 to #53 no attempt was made to analyse the hydrogen.

— No analysis performed.

TABLE XI

Rate of formation of carbon dioxide at 152.5°C and relative intensity = 1

Run	Pressure (mm Hg)	[C ₆ H ₅ COOH] x 10 ⁵ (mole liter ⁻¹)	Time (sec)	R _{CO₂} x 10 ⁶ (mole hr ⁻¹)	log ₁₀ R _{BA}	log ₁₀ Rate _{CO₂}
63	0.216	0.815	6000	2.79	-5.0888	-5.5544
64	0.214	0.808	3600	2.95	-5.0926	-5.5302
65	leaking					
66	1.191	4.200	5000	1.89	-4.3747	-5.7235
67	1.025	3.868	4000	2.23	-4.4125	-5.6517
68	0.288	1.087	4500	1.81	-4.9637	-5.7423
69	1.730	6.528	4600	1.67	-4.1853	-5.7773
70	1.685	6.355	4000	2.14	-4.1967	-5.6696
71	1.670	6.310	2000	2.58	-4.2000	-5.5884
72	leaking					
73	0.073	0.276	3600	1.38	-5.5581	-5.6021
74	0.216	0.816	4000	1.52	-5.0883	-5.7645
75	0.208	0.785	1500	1.71	-5.1051	-5.7133
76	0.206	0.778	850	1.63	-5.1090	-5.7305
77	1.235	4.660	1200	1.21	-4.3316	-5.9172
78	0.060	0.226	2500	0.97	-5.6459	-5.7352
79	0.456	1.712	1800	1.80	-4.7665	-5.7447

TABLE XII

Effect of Temperature on rate formation of CO₂ at relative intensity = 1

Run	Pressure (mm Hg)	[C ₆ H ₅ COOH] x 10 ⁵ (mole liter ⁻¹)	Time (sec)	R _{CO₂} x 10 ⁶ (mole hr ⁻¹)	Temperature °C	log ₁₀ R _{CO₂}	$\frac{1}{T} \times 10^3$ (°K ⁻¹)
62	0.416	1.156	7200	4.38	305.3	-5.3270	1.7286
68	0.288	1.087	4500	1.81	152.5	-5.7423	2.3479
80	0.206	0.863	3600	1.03	109.9	-5.9872	2.6102
81	0.386	1.284	2400	2.72	208.9	-5.5654	2.0742

TABLE XIII

Thermal Reactions

Thermal Run **	Temperature (°C)	Pressure (mm Hg)	Mole hr ⁻¹ x 10 ⁸		
			CO ₂	CO	H ₂
1*	150	0.050	191.0	-	-
2	150	0.050	21.0	-	-
3	150	0.050	10.0	-	-
4	150	0.050	7.0	-	-
5	150	0.050	8.0	2.0	1.65
6	202	0.065	6.0	3.6	2.75
7	214	0.065	4.0	-	-
8	207	0.068	7.0	4.0	1.08
9	245	0.300	13.0	5.3	1.15
10	310	0.488	16.0	-	-
11*	310	0.445	57.0	-	-
12	310	0.426	25.0	-	-
13	150	0.050	5.0	-	-
14	150	0.080	8.0	-	-

* Reactions were carried out after the reactor had been exposed to air.

** The thermal runs were performed at various times throughout the experiments.

- No analysis performed.

FIGURE 1

Diagram of Apparatus

T	Glass stopcocks
ST	Springham stopcocks
SH	Sensing head
BU	Balance unit
R	Reactor
EF	Electric fan
S _{BA}	Benzoic acid storage
AF	Air furnace
U	U-traps
C	Cold traps
M	Manometers
MG	McLeod gauge
MD	Mercury diffusion pump
TP	Toepler pump
VPC	VPC sampling tube
SR	Solid sampling tube
SC	Calibrated gas burette
O	CuO oxidation chamber
A,B	Compartments

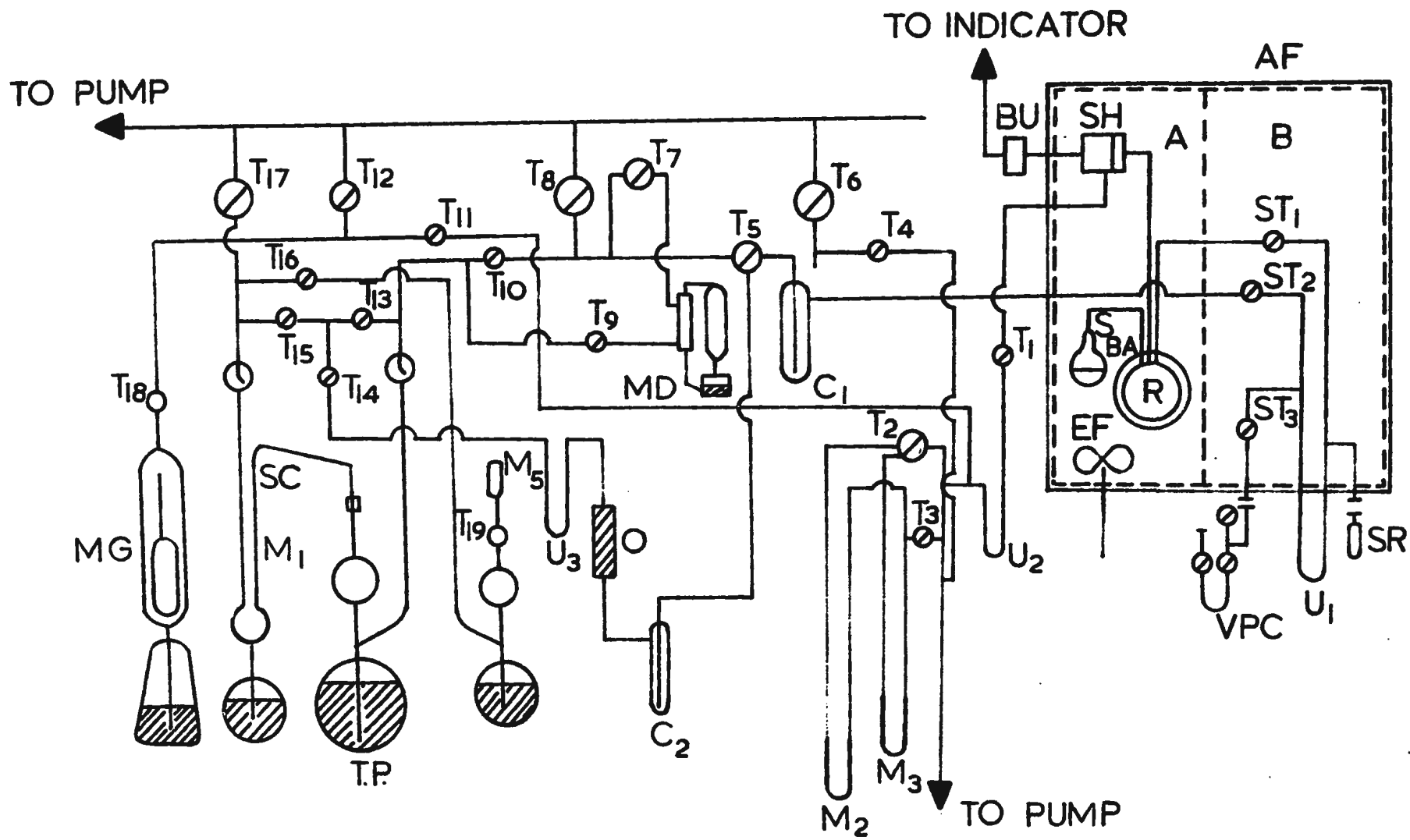


FIGURE 2

Reactor and thermocouples

⊙ Location of thermocouples

2

FIG.2

REACTOR VESSEL

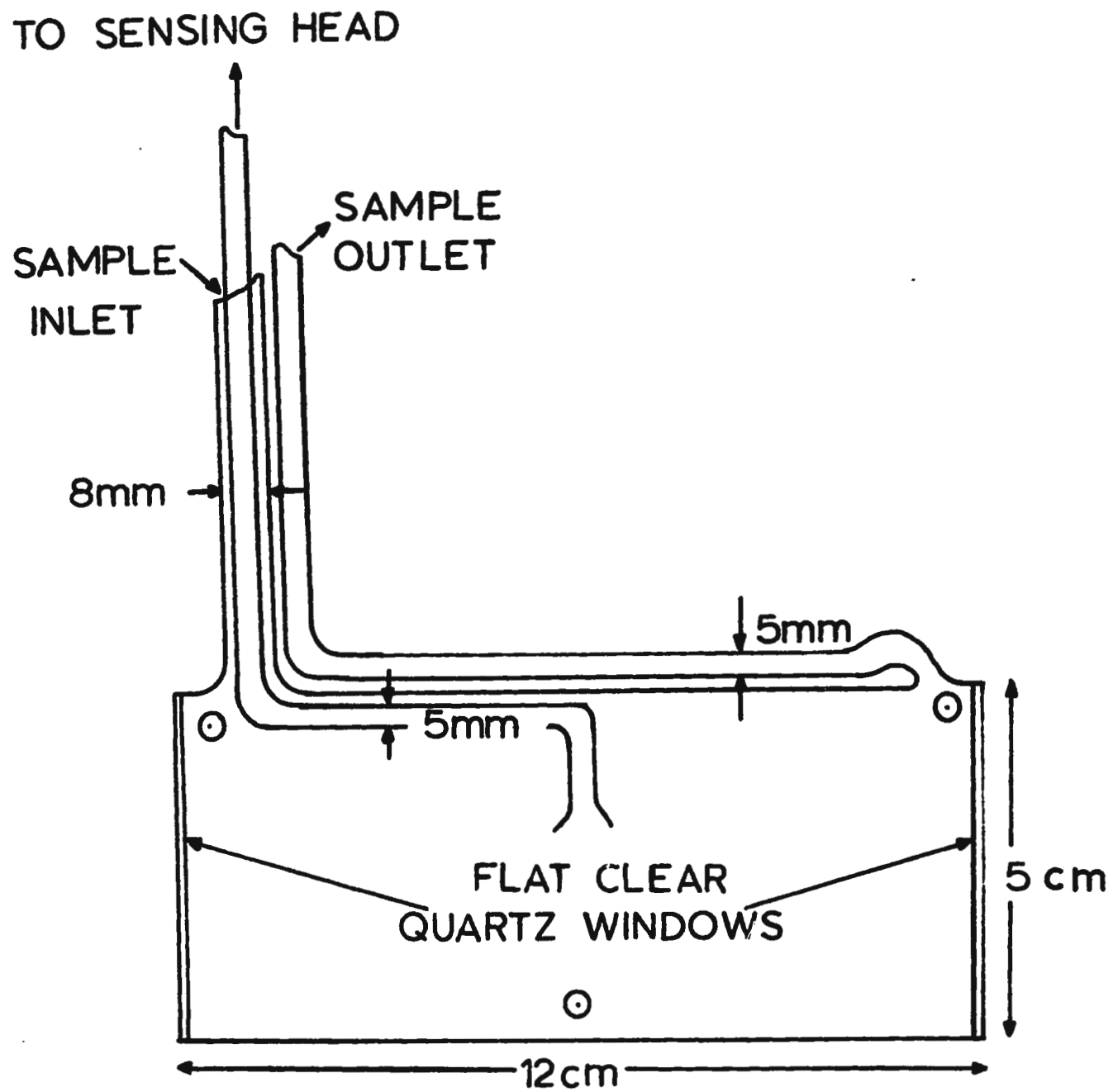


FIGURE 3

Diagram of sensing head

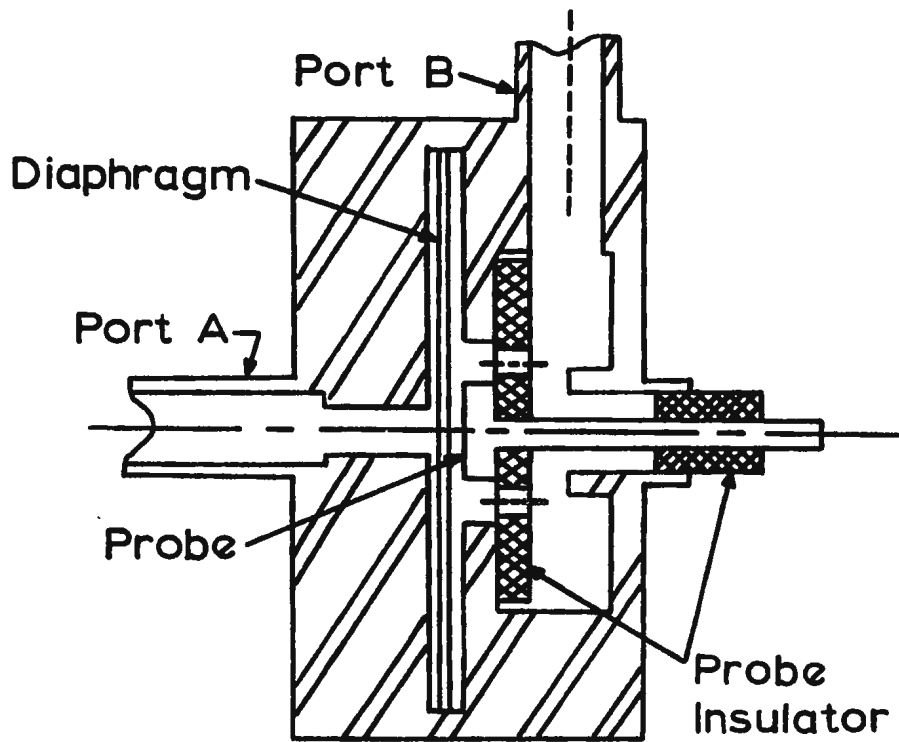


FIGURE 4

Electronic schematic of balance unit

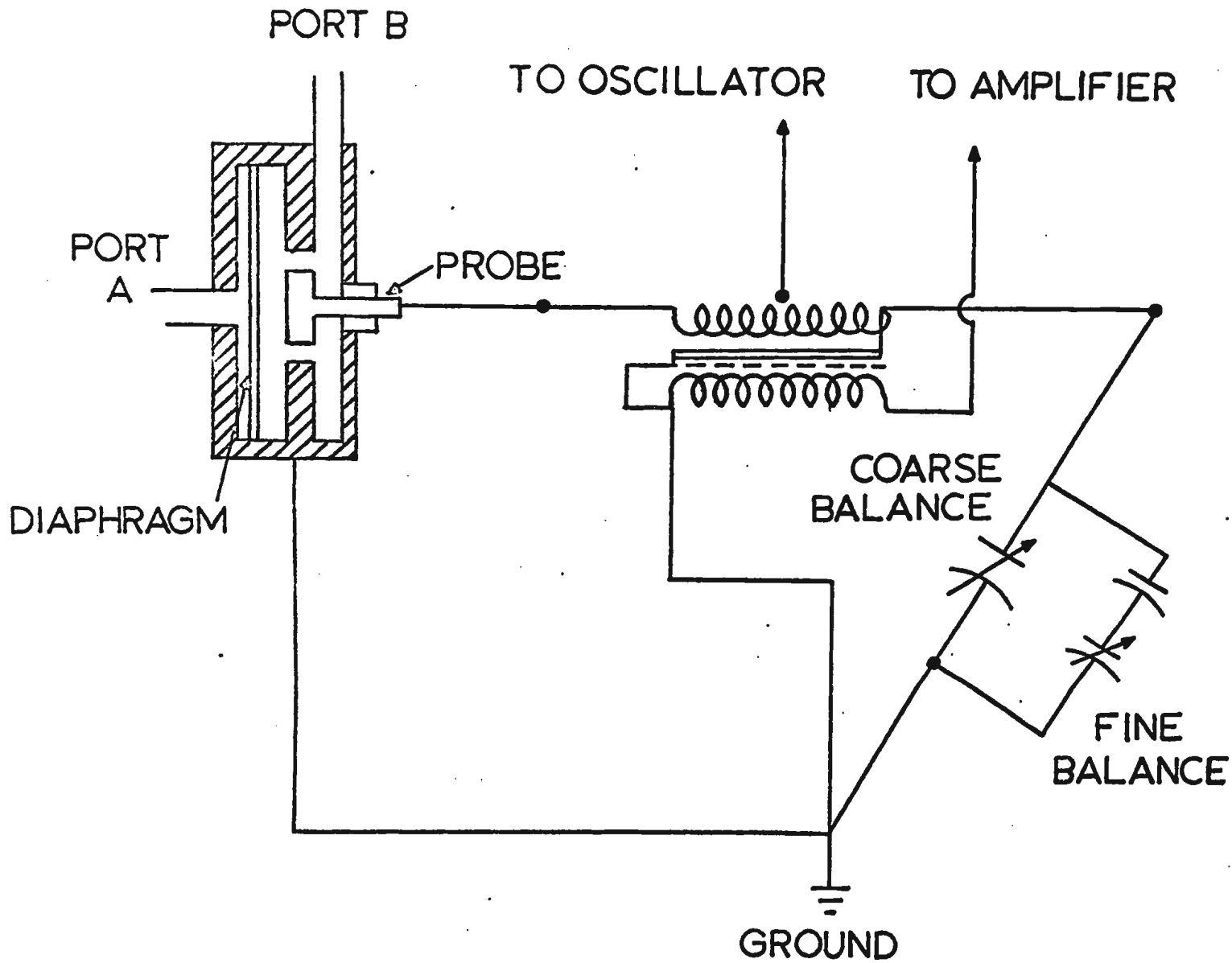


FIGURE 5

Optical Arrangement

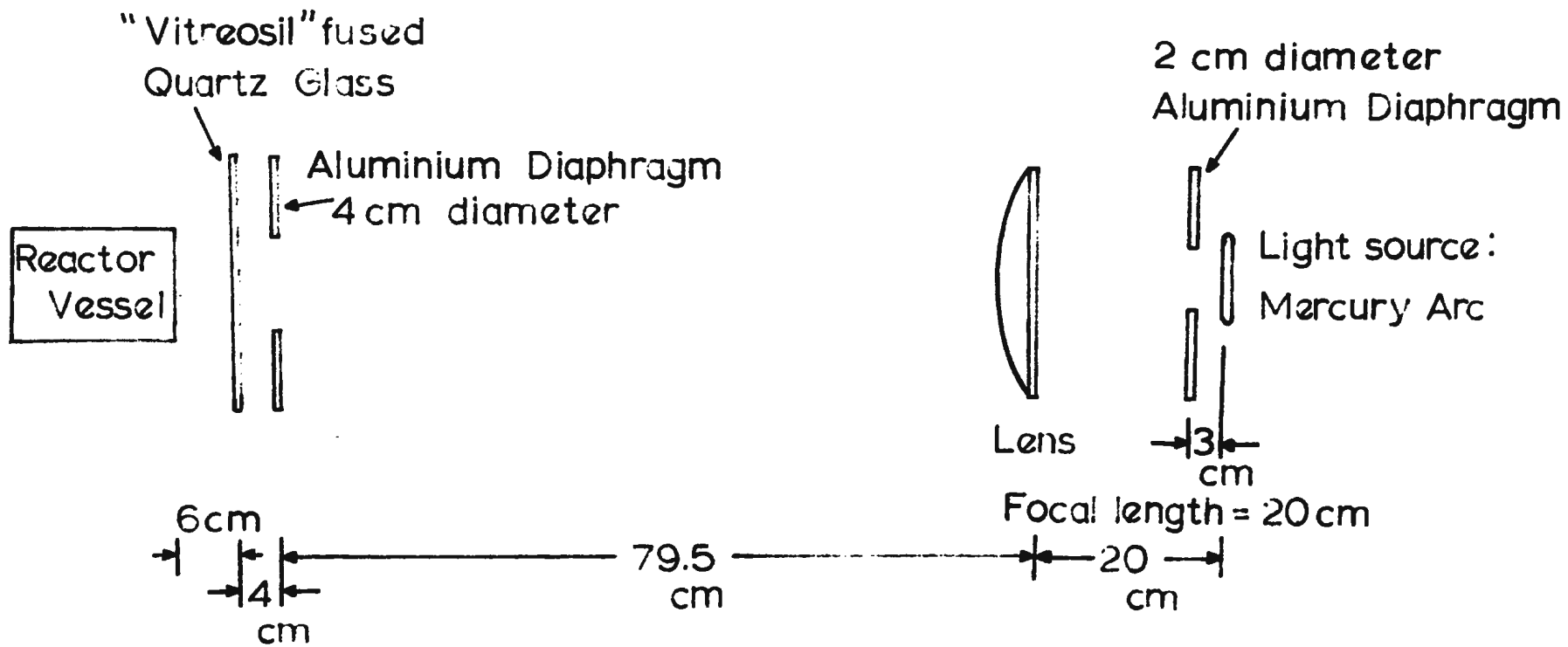
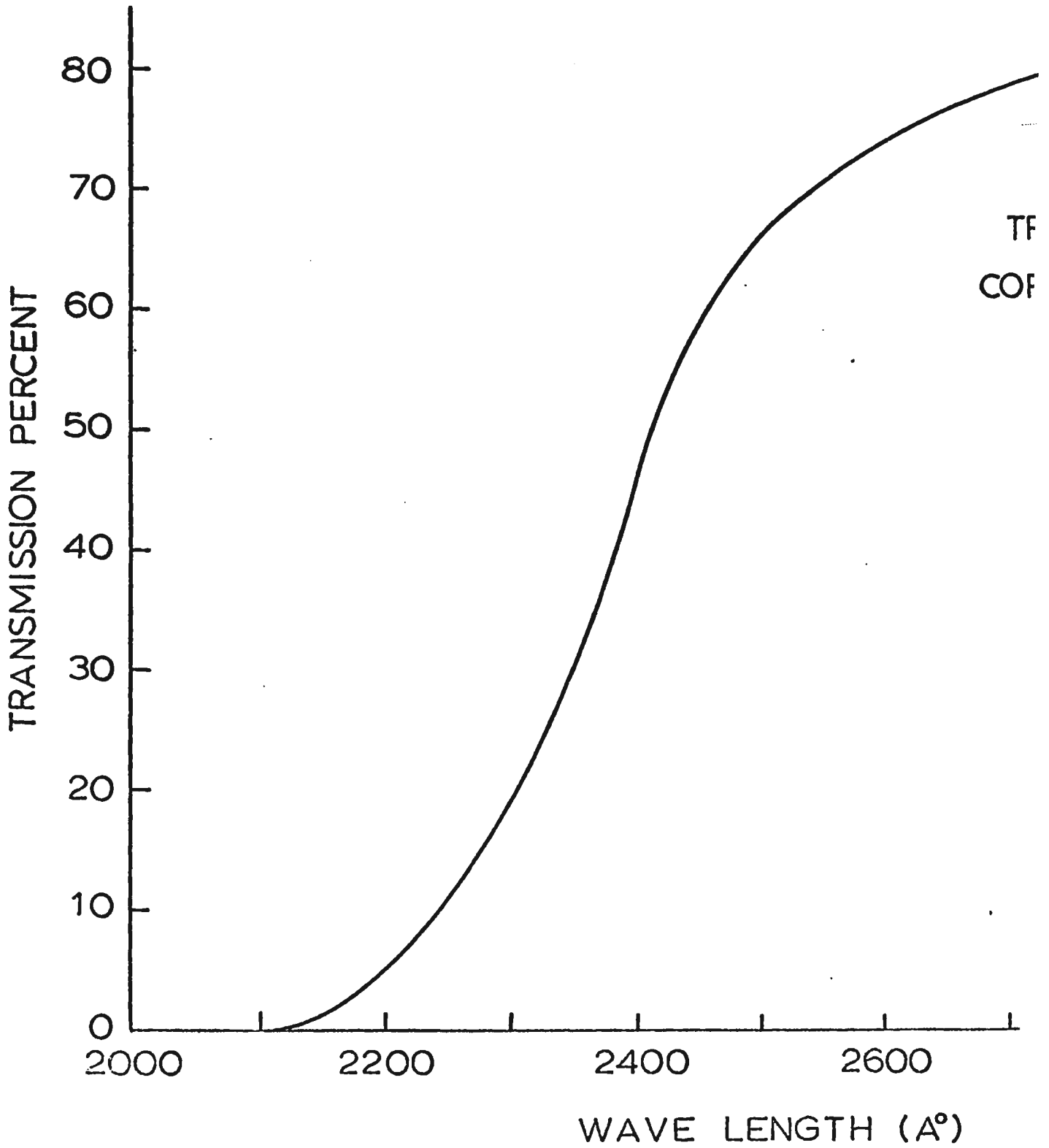
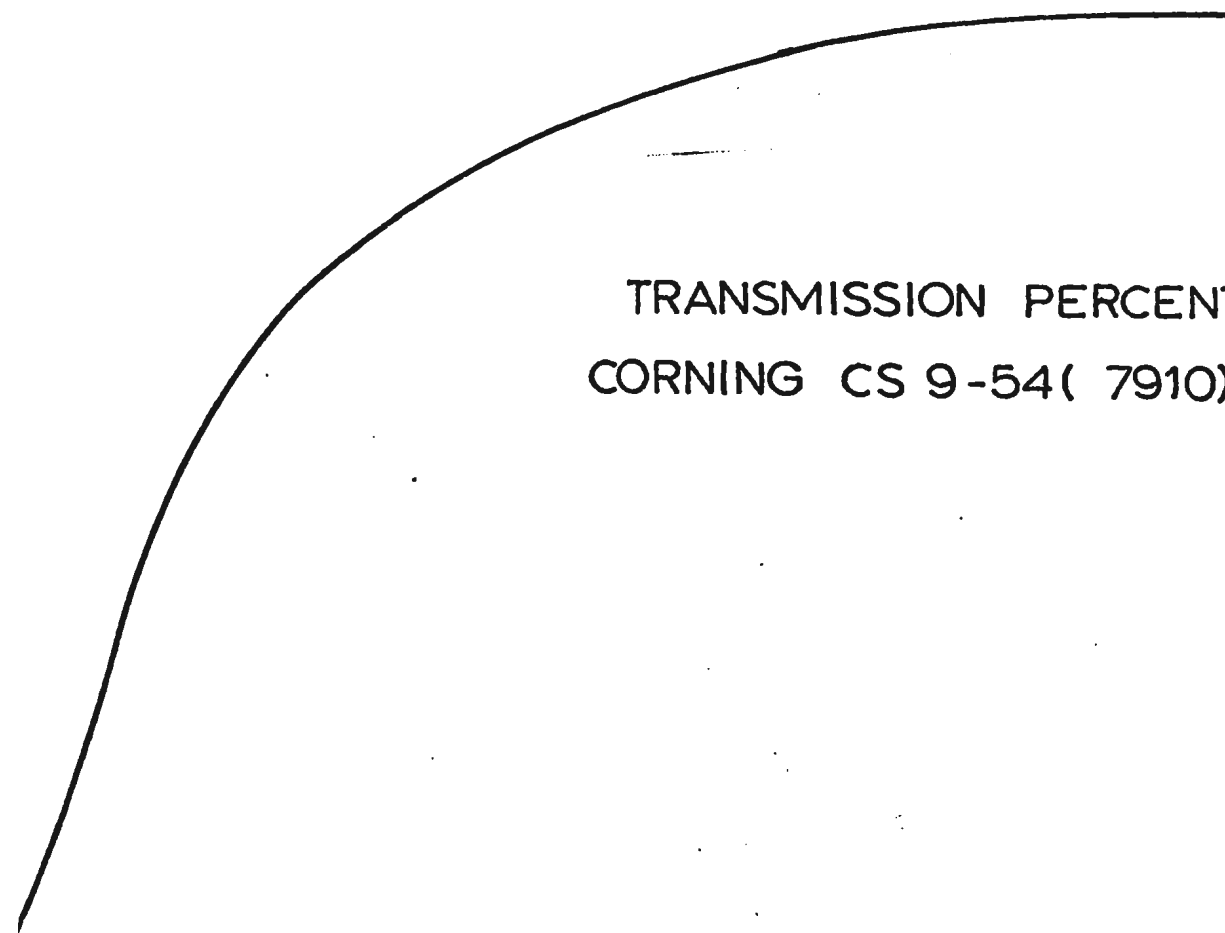


FIGURE 6

Percent transmission of Corning CS 9-54 filter



TRANSMISSION PERCENT OF
CORNING CS 9-54(7910) FILTER



2400 2600 2800 3000

WAVE LENGTH (Å)

FIGURE 7

Mass spectrum of the non-condensable gases from
experiment # 62

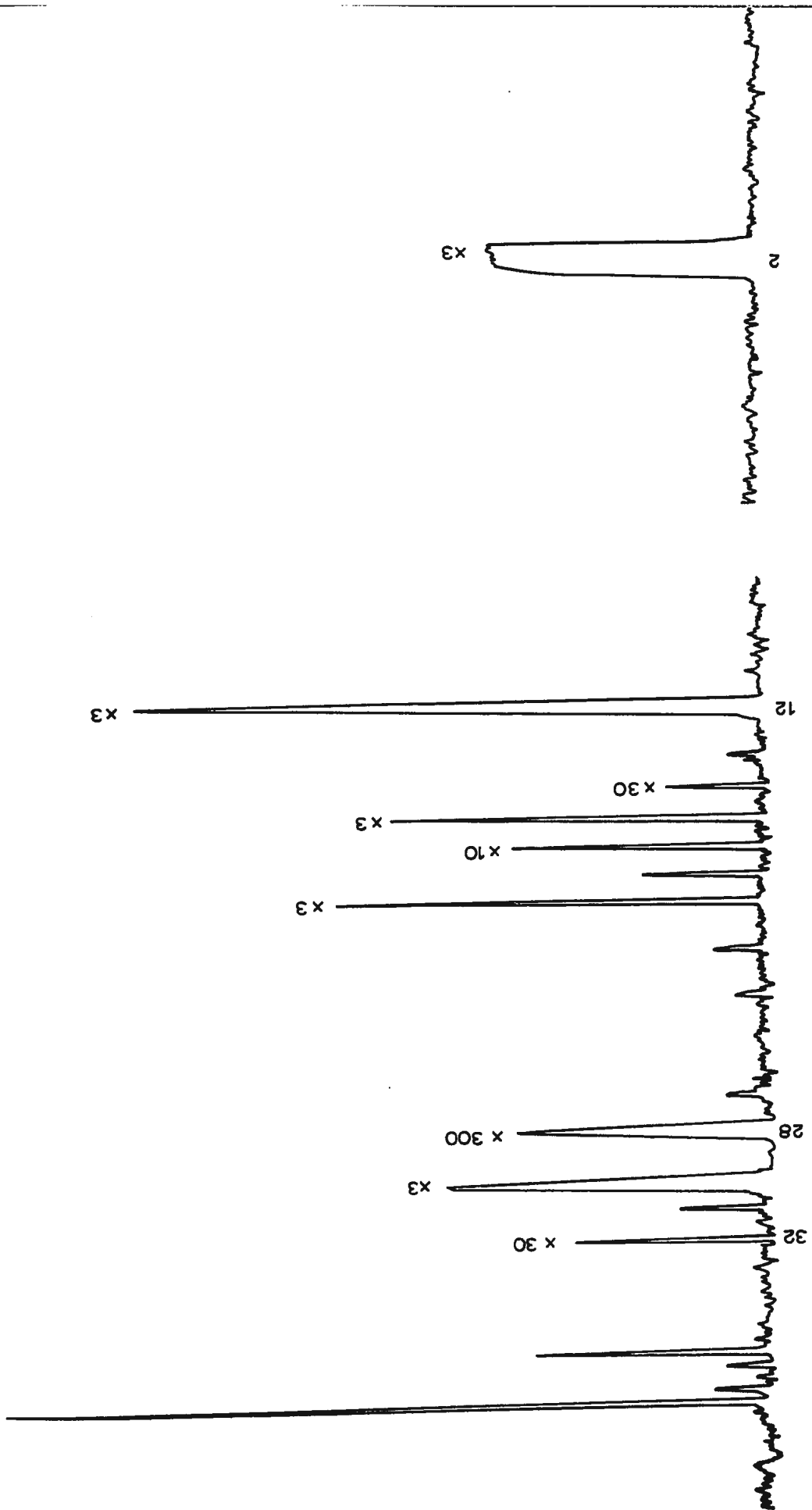
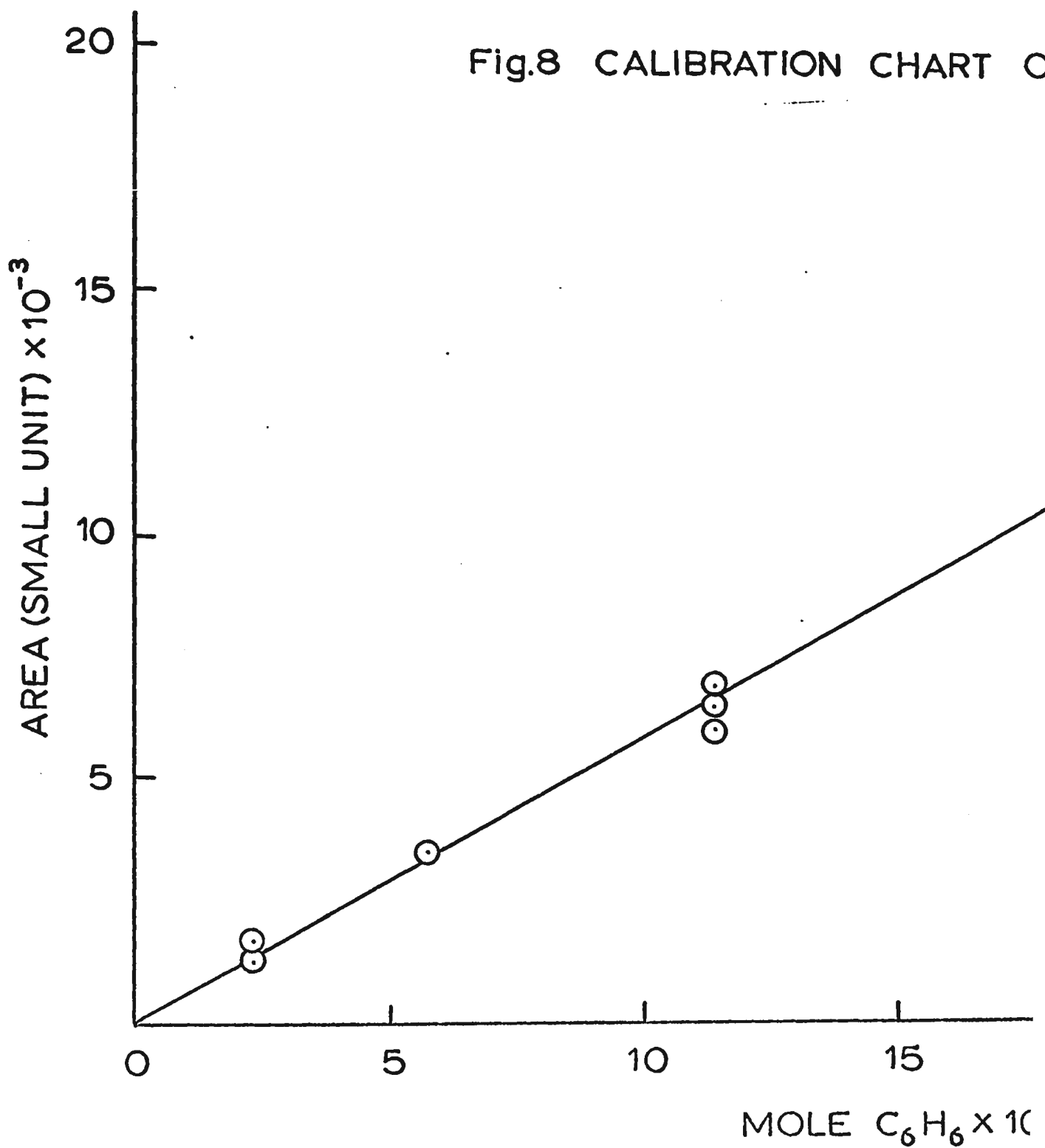


FIGURE 8

Calibration chart of benzene

Fig.8 CALIBRATION CHART OF



3RATION CHART OF BENZENE

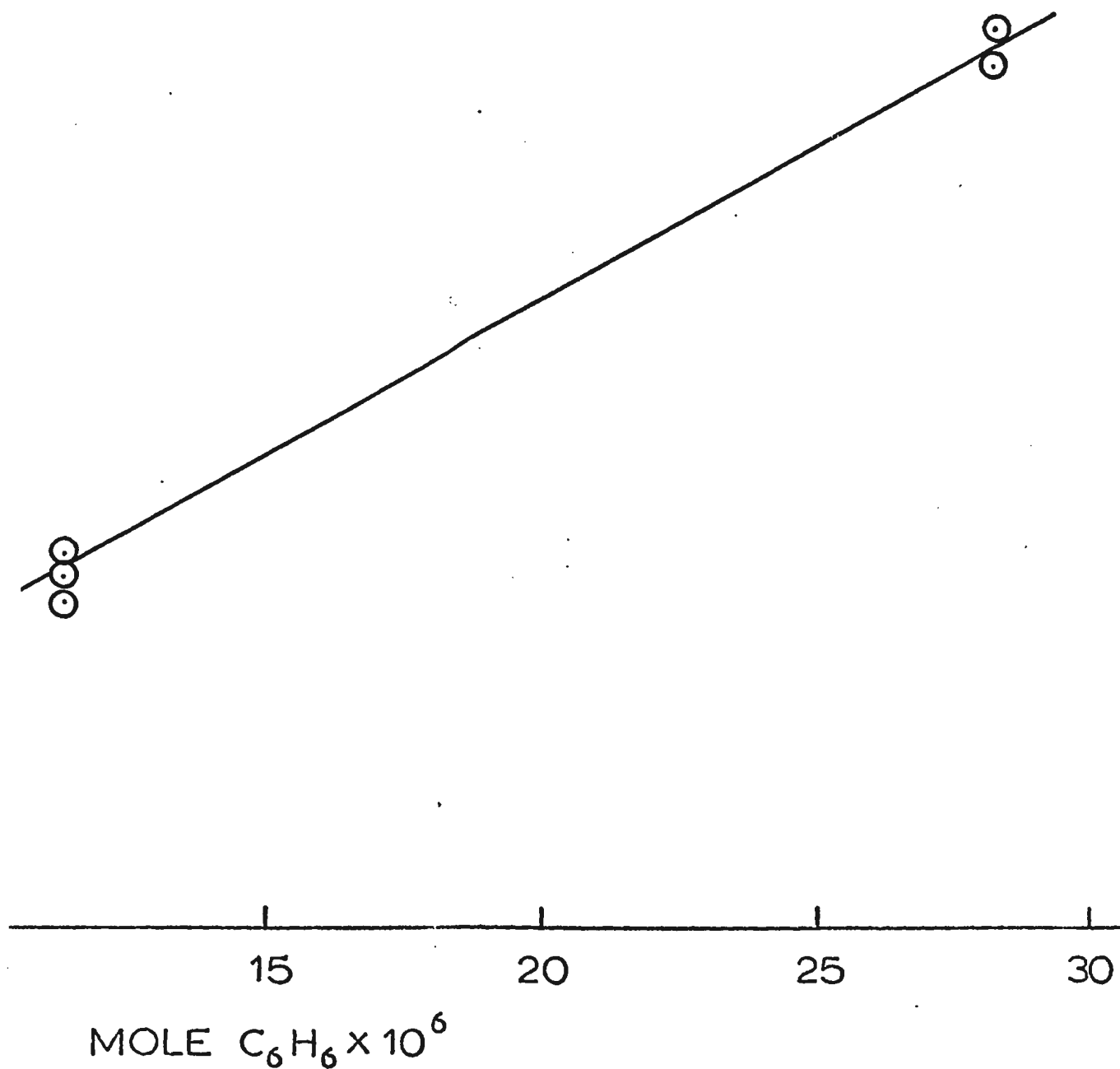


FIGURE 9

Plots of rates of CO_2 and CO formation against relative light intensity at 150°C and 205°C .

- Rate at 150°C
- ▲ Rate at 205°C

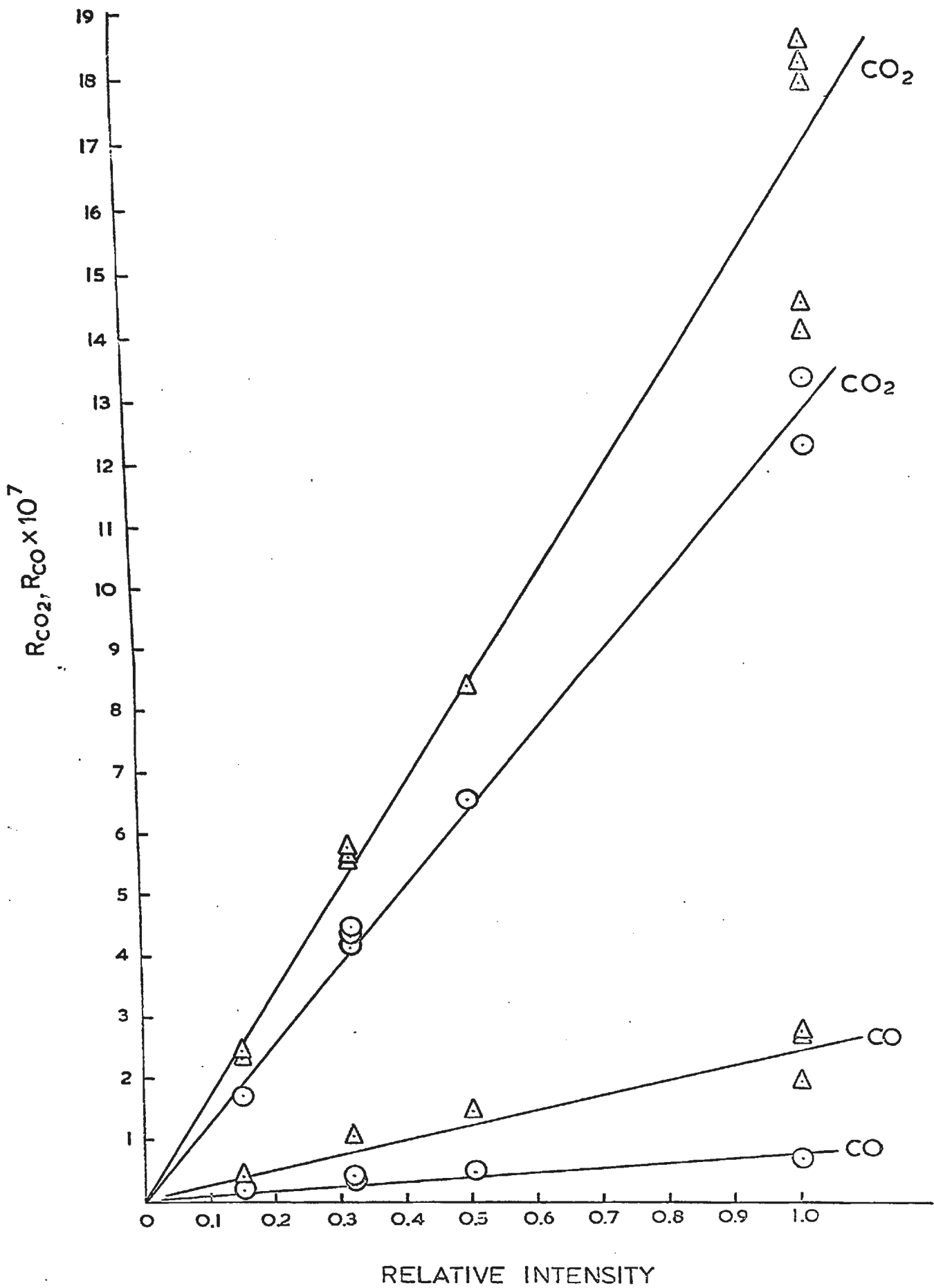


FIGURE 10

Plots of log rate of CO₂ formation against log relative light intensity at 150°C and 205°C.

- ⊙ Rate at 150°C
- ▲ Rate at 205°C

FIGURE 11

Plots of log rate of CO formation against log relative light intensity at 150°C and 205°C.

- Rate at 150°C
- ▲ Rate at 205°C

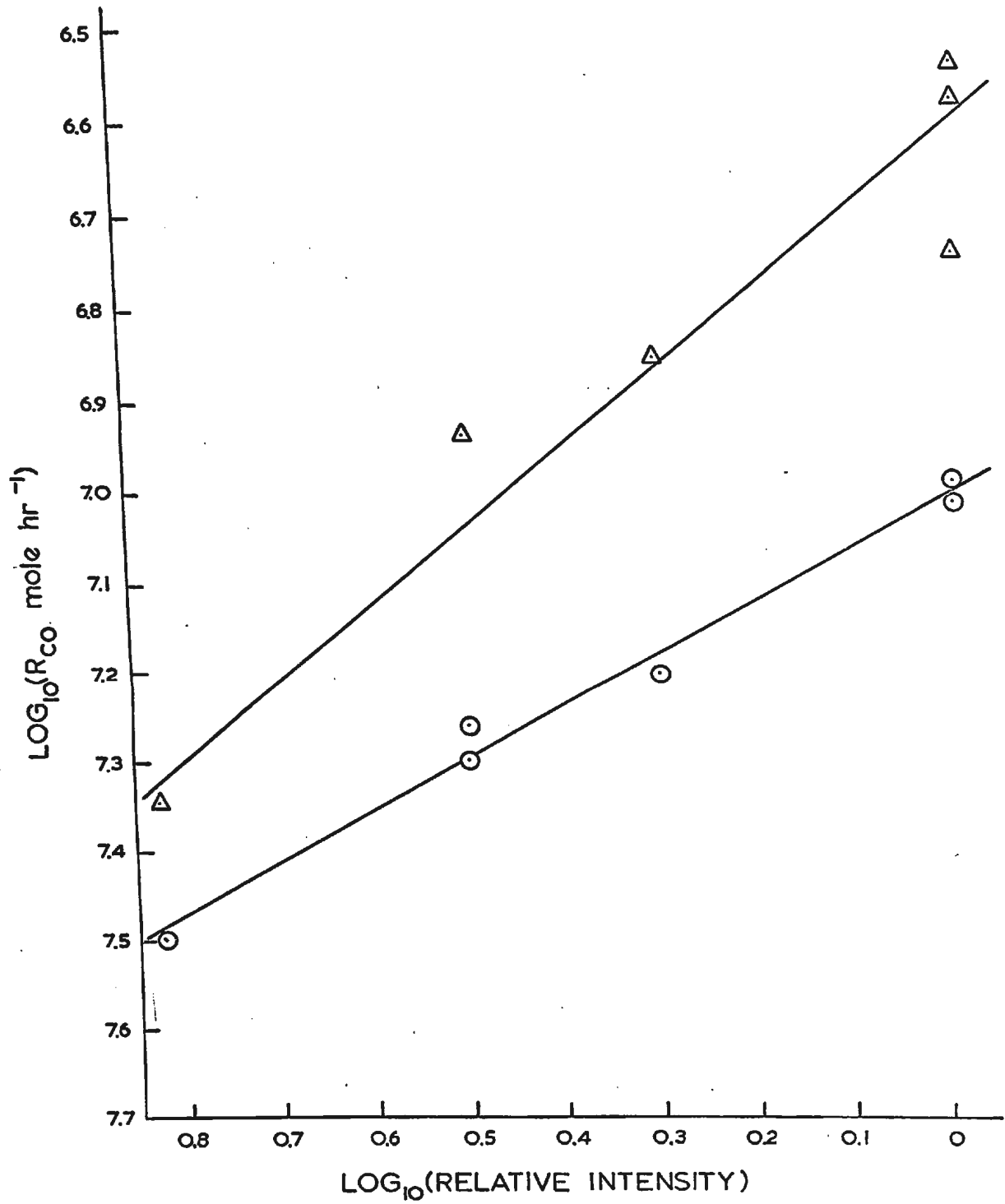


FIGURE 12

Plot of rate of CO_2 formation against concentration of benzoic acid at 152°C

- Experiments were carried out with Springham stopcocks
- △ Experiments were carried out with greased stopcocks

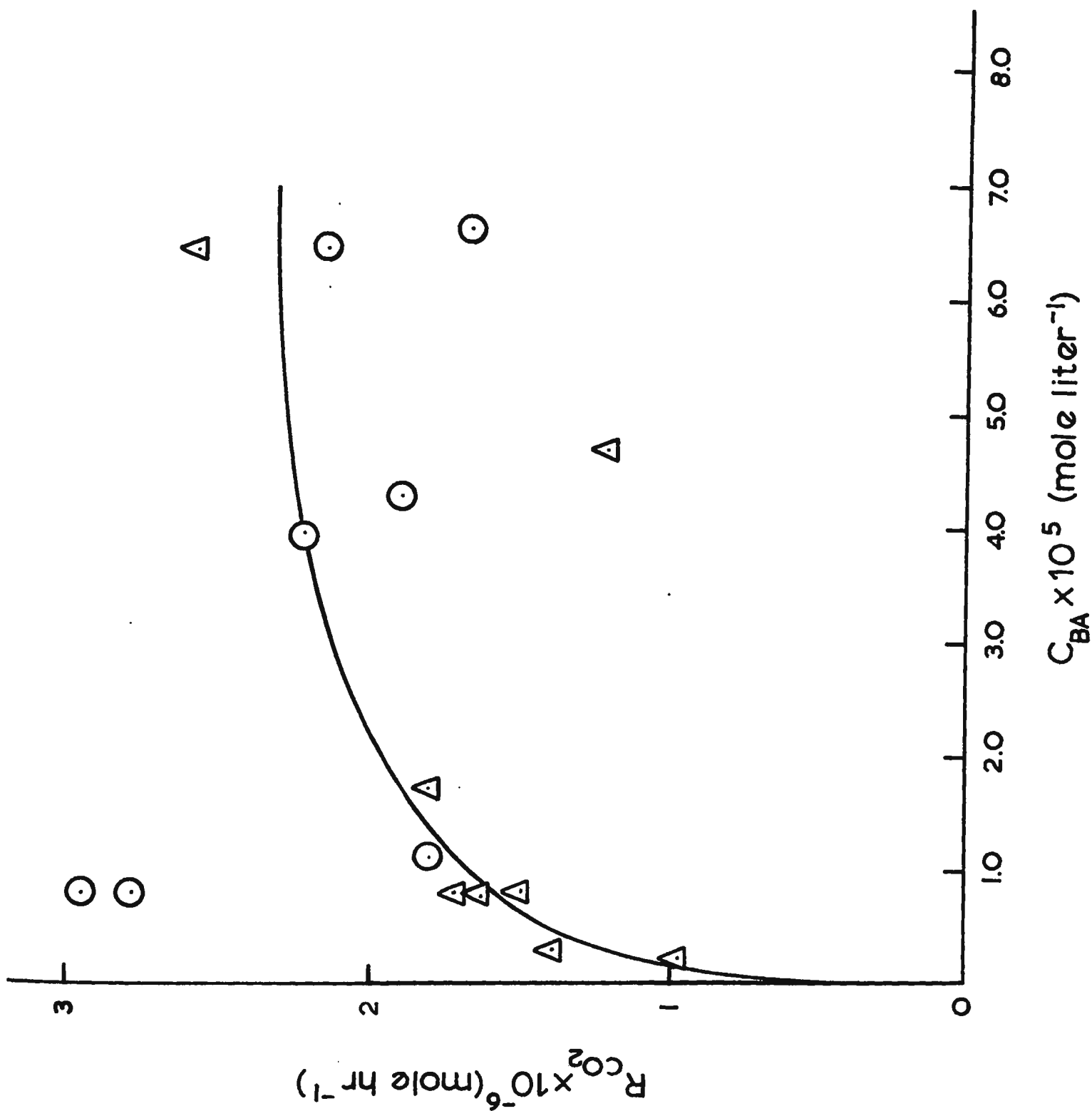


FIGURE 13

Plot of log rate of CO₂ formation against
log concentration of benzoic acid at 152°C

A Data were corrected by considering the
light intensity absorbed.

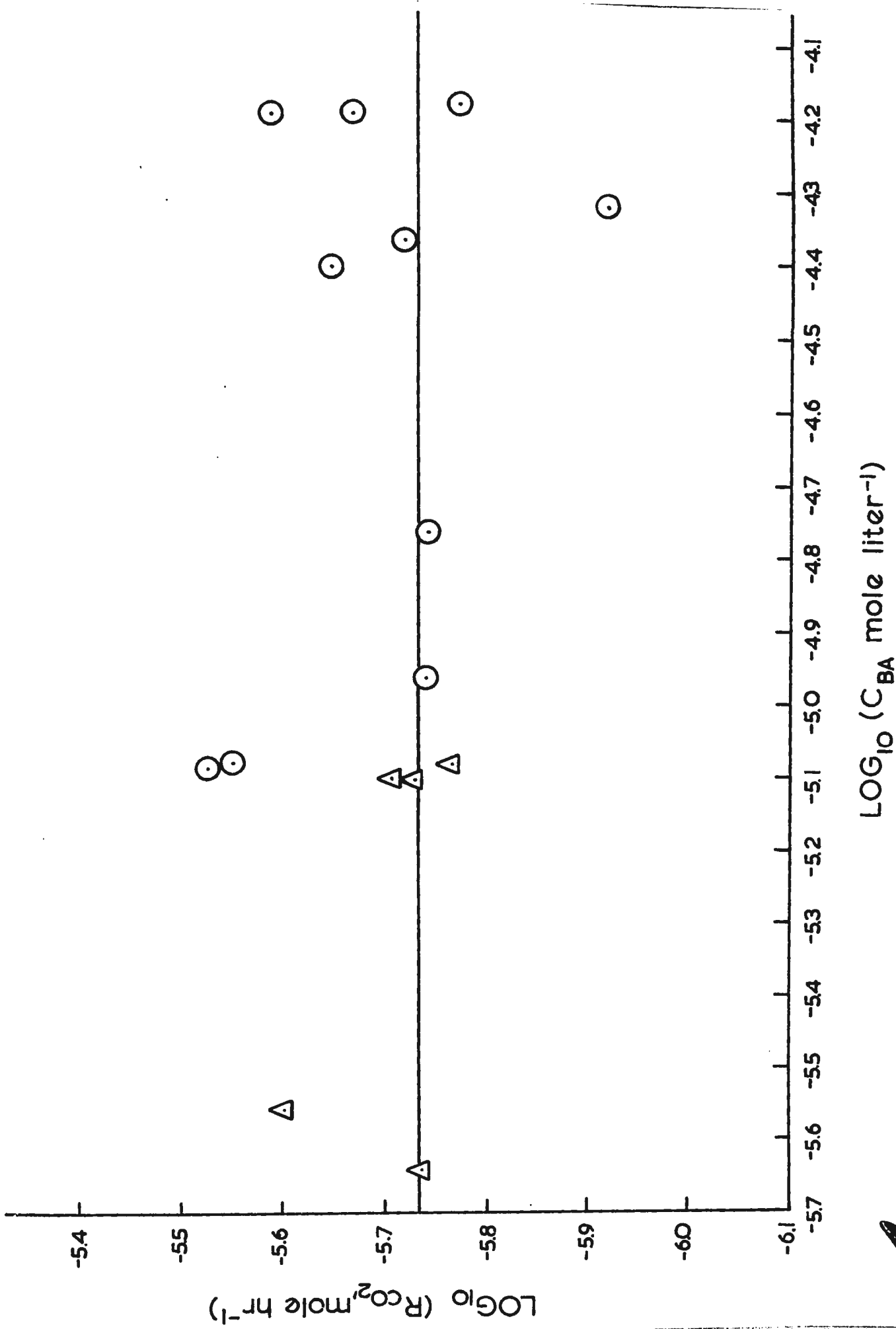


FIGURE 14

Plot of log rate of CO₂ formation against
1/T at constant light intensity and constant
benzoic acid concentration.

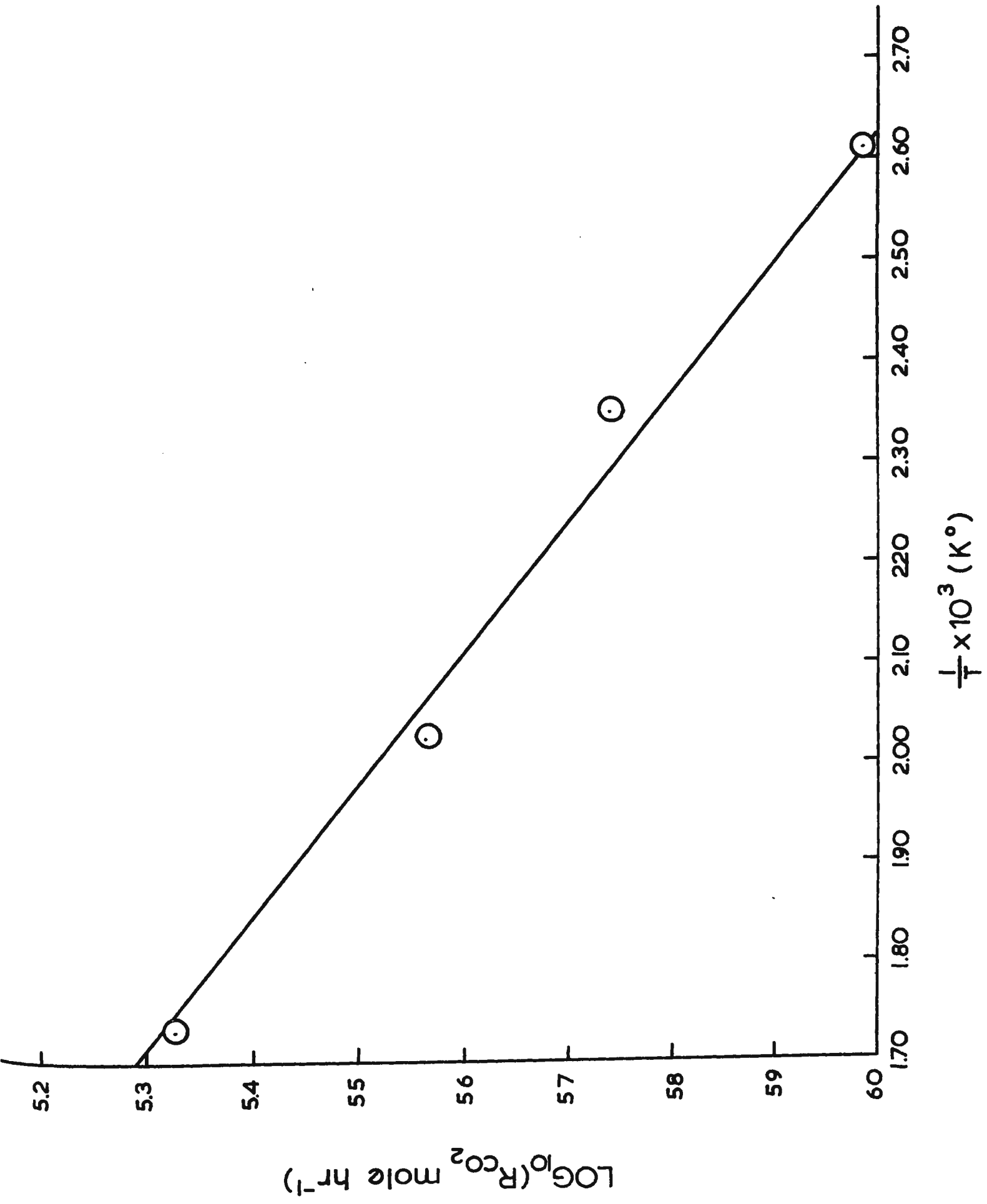
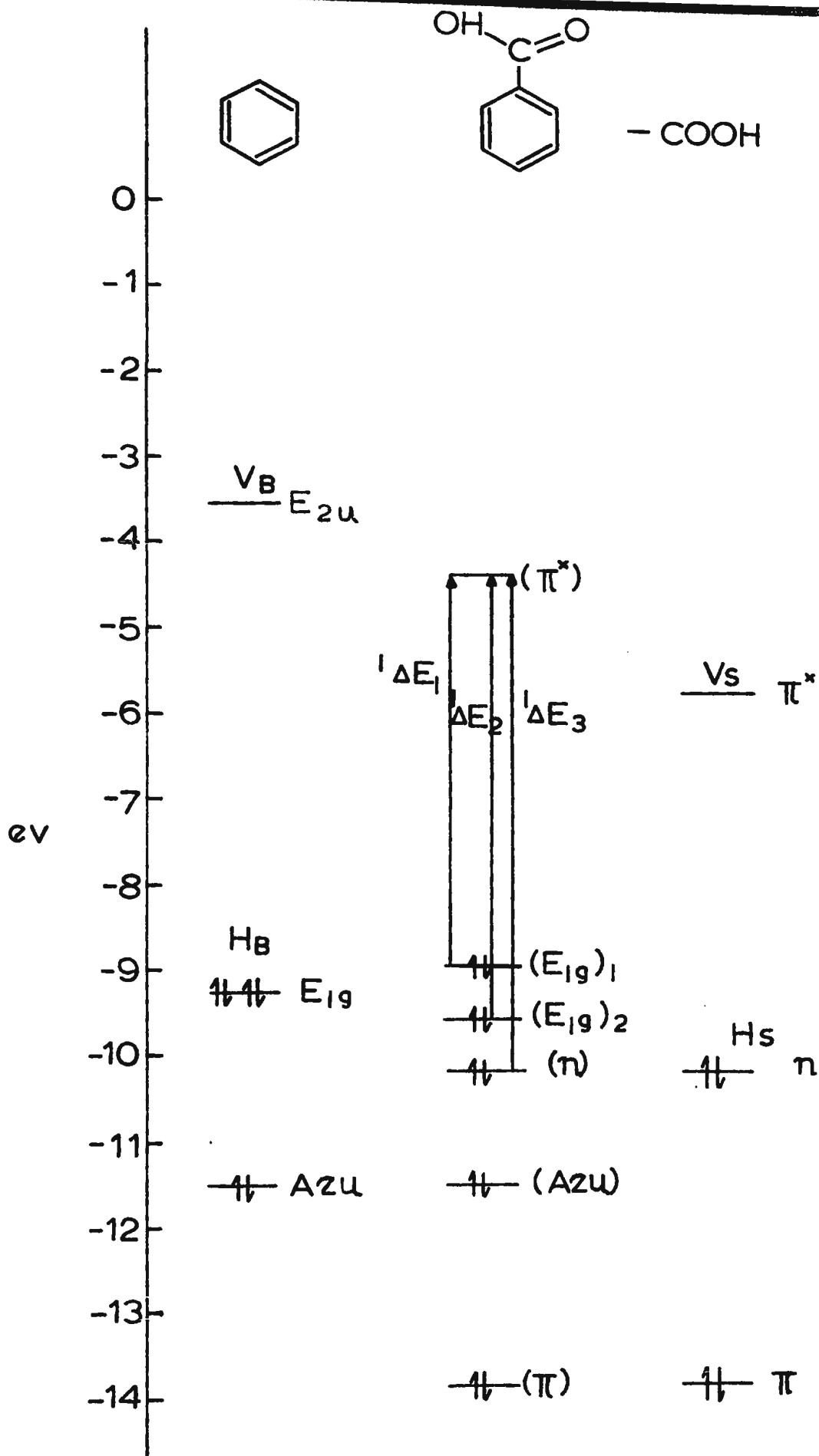


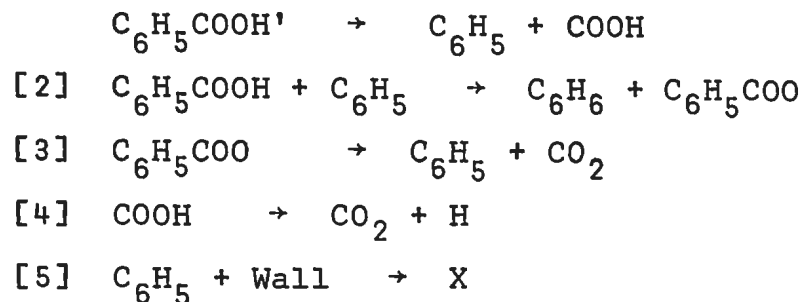
Figure 15

π -electron energy level diagram of benzoic acid



APPENDIX

Estimates of heats of reaction



Reaction [11] has already been discussed on page 52.

For reactions [2] and [3], the heats of reaction are estimated from the following heats of formation.

$$\begin{aligned} \Delta H_{\text{fo}}(\text{H}) &= 52 \quad \text{kcal mole}^{-1} * \\ \Delta H_{\text{fo}}(\text{CO}_2) &= -94.1 \quad \text{kcal mole}^{-1} * \\ \Delta H_{\text{fo}}(\text{C}_6\text{H}_6) &= 19.8 \quad \text{kcal mole}^{-1} * \\ \Delta H_{\text{fo}}(\text{C}_6\text{H}_5) &= 80 \quad \text{kcal mole}^{-1} \ddagger \\ \Delta H_{\text{fo}}(\text{COOH}) &= -54 \quad \text{kcal mole}^{-1} * \end{aligned}$$

$$\text{and } \Delta H_{\text{fo}}(\text{C}_6\text{H}_5\text{COOH}) = -60.9 \quad \text{kcal mole}^{-1} \dagger$$

This would lead to a ΔH° of -2.3 and -11.0 kcal mole⁻¹ for reactions [2] and [3] respectively.

Reaction [4] has been mentioned on page 55.

In reaction [5], the critical point may be the rate of diffusion of radical, C_6H_5 , to the wall. The activation energy for diffusion is very small.

* S.W. Benson, J. Chem. Ed. 42, 502 (1965).

‡ A.S. Rodgers, D.M. Golden, and S.W. Benson, Ber. Bunsenges. Physik. Chem. 72, 253 (1968).

† J.D. Cox, Tetrahedron 18, 1337 (1962).

Comments by Dr. G. Semeluk

P. 32, regarding wall termination and diffusion -

It is difficult to accept the supposition offered which suggests a change in mechanism. Some idea of the importance of wall termination may have been obtained by varying the diameter of the irradiating beam, and changing (total) pressure. Large changes in chain length would occur if wall terminations were important.

p. 47, Fluorescence lifetime -

It is not clear who, if anyone, has observed fluorescence from benzoic acid. If internal conversion is as efficient as is implied, fluorescence may not be "observable" at any reasonable pressure. It is difficult to reconcile the very low quantum yield inferred, with a chain reaction. A directly measured quantum yield would be invaluable here.

